2000

The morphology and film formation of low Tg core-shell latex particles

Karl M. Seven
Lehigh University

Seven, Karl M.

The Morphology and Film Formation of Low Tg Core-Shell Latex Particles

January 2001

THE MORPHOLOGY AND FILM FORMATION OF LOW T_g CORE-SHELL LATEX PARTICLES

By

Karl M. Seven

A Research Report
Presented to the Graduate and Research Committee
of Lehigh University
in Candidacy for the Degree of
Master of Science

in
Polymer Science and Engineering

Lehigh University

2000

CERTIFICATE OF APPROVAL

This research report, submitted by Karl M. Seven, is accepted in partial fulfillment of the requirements for the degree of Master of Science in Polymer Science and Engineering.

11/30/2000
Date

Professor Andrew Klein,
Faculty Advisor

Dr. Eric S. Daniels,
Research Scientist

Dr. Victoria L. Dimonie,
Research Scientist

Professor M. S. El-Aasser,
Chairman of Department

ACKNOWLEDGEMENTS

I would like to thank the following people for their assistance during this research project:

Professor Andrew Klein, Professor Mohamed S. El-Aasser, Dr. Eric Daniels, Dr. Victoria Dimonie and Ms. Olga Shaffer for advice and guidance.

Friends, colleagues, and administrative staff members for assistance.

My mother, father, sister and brother-in-law for love and family support.

The Emulsion Polymers Institute Industrial Liaison Program for financial support.

TABLE OF CONTENTS

LIST OF TABLES

LIST OF FIGURES

ABSTRACT

A series of low T_g composite latexes with varying compositions were synthesized by seeded batch emulsion polymerization and semi-continuous seeded emulsion polymerization methods. The seed latex consisted of poly(lauryl methacrylate) (PLMA) and the shell was comprised of a copolymer of poly(2-ethylhexyl methacrylate) (P2-EHMA) and benzyl methacrylate (BM). Potassium persulfate was used as the water-soluble initiator, however in one series of polymerizations, the oil-soluble initiator 2,2'-azobis(isobutyronitrile) (AIBN) was used for comparative studies. The effect of the initiator type and lightly crosslinking the P2-EHMA phase with ethylene glycol dimethacrylate (EGDMA) was investigated with respect to glass transition measurements (T_g), mechanical properties and film surface morphology of dried latex films.

It was found that in most cases the measured volume-average latex particle diameters (D_v) were larger than the expected diameters based on a theoretical calculation. Latex particle sizes measured by capillary hydrodynamic fractionation (CHDF) were smaller than those measured by dynamic light scattering (DLS) techniques. Particle size distributions of the seed PLMA latex were quite monodisperse and monodispersity was maintained after the second stage polymerizations.

The results of glass transition (T_g) measurements on the films of composite latexes synthesized here indicate very little change in T_g as compared to the measurements made on PLMA homopolymer and P2-EHMA/BM copolymer. Multiple T_g values were obtained for the dried latex films. The results obtained indicated that these two polymers are not very miscible with one another. The glass transitions

obtained from the semi-continuous process were broader than those obtained from a batch type seed/swell polymerization. In the seed/swell process the seed latex is first swollen with the shell monomer and subsequently polymerized around the seed. The results of T_g measurements may indicate that greater miscibility between the two phases is achieved in the semi-continuous process.

Latex films of the following compositions (PLMA/P2-EHMA) were obtained by either latex blending or core/shell synthesis techniques: 0/100, 25/75,. 33/66, 50/50, 66/33, 75,25. The mechanical properties of these films were measured by an Instron tensile testing machine. The toughness of both the latex blends and composite latexes varied with composition ratio. Generally, the mechanical properties of the dried composite latex films were higher for the 33/66 and 25/75 than for the corresponding 33/66 and 25/75 latex blends. Whereas the mechanical properties of the latex blends for the 66/33 and 50/50 compositions were higher than for the composite latexes. The mechanical properties obtained for the 33/66 wt% series of latexes overall were superior to those obtained by simple physical blending of PLMA and P2-EHMA copolymer except in the case where EGDMA crosslinker was added. The greatest improvement in properties as compared to the latex blends was seen with the latex synthesized by the seed/swell technique. Latexes synthesized by semi-continuous polymerization and latexes synthesized using AIBN as initiator showed only modest improvements in the mechanical properties. For these films, the toughness and elongation at break were relatively close to those obtained from latex blends except for the tensile stress at break. These results may have been due to incomplete coalescence of the dried latex films which were evident in the atomic force microscopy (AFM) images. Generally, toughness

appeared to increase as the composition ratio (core/shell) increased for both blend and composite latexes.

Results of atomic force microscopy (AFM) studies were employed to correlate physical properties with latex film structure on a microscopic scale. The images obtained for the film prepared via the seed/swell process indicated microstructure and rather complete coalescence. Voids or gaps between latex particles were qualitatively smaller than in the other films, all of which led to an increase in the mechanical film strength compared to the other films tested.

CHAPTER 1

INTRODUCTION

1.1 Low T_g Latex

Emulsion polymerization is a particularly practical and convenient method of synthesizing latex in a form that is suitable for formulation into water-borne products to be used in adhesives and coatings. Industry is seeking to replace currently established solvent-borne adhesives and coatings with suitable latexes due to increasing environmental problems associated with organic solvent-based systems. For example, the desire to remove organic solvents in pressure-sensitive adhesives is particularly strong since these products are usually solvent based. Generally, pressure-sensitive adhesives are based on low T_g polymer systems typically in the range of -40 to –50 °C. In most cases, they are copolymers prepared using either n-butyl acrylate or 2-ethylhexyl acrylate as the principal monomer.

Figure 1 shows the appropriate glass transition temperature range for a variety of end-use applications of acrylic-type emulsion polymers. The glass transitions of the polymers used in this research are in the low T_g range corresponding to those commonly used in applications such as pressure-sensitive adhesives. Pressure-sensitive adhesives must be soft and tacky, whereas floor polishes must be hard and tough to withstand being stepped on and non-adherent to objects placed on them.[1]

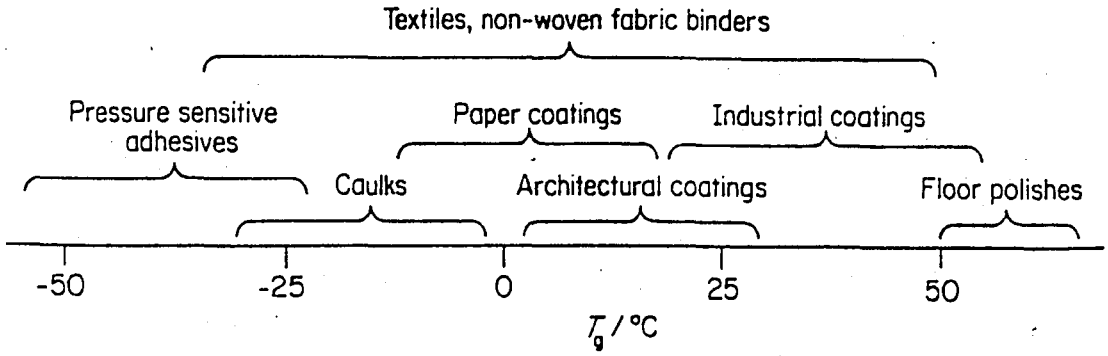

Figure 1-1: Polymer Glass Transition Temperatures of Acrylic Latexes Appropriate for Various Product Applications.[1]

This research focused on the morphology, film formation and mechanical properties of a low T_g emulsion polymer system based on poly(lauryl methacrylate) (PLMA) with a T_g of –65 °C and poly(2-ethylhexyl methacrylate) (P2-EHMA) with a T_g of –10 °C. Therefore, in this system both the core and shell polymer were low glass transition materials.

1.2 Core-Shell Latex

Composite latex particles with differing morphologies can be synthesized by an emulsion polymerization process in the presence of a seed latex. Usually a second type of monomer is polymerized in the presence of the seed particles. The resulting latexes often have a particle structure with the initially polymerized polymer located at the center of the particle and the later formed polymers bound to an outer shell of the seed latex forming a "core-shell" type morphology.[2] Since most polymer pairs are not compatible, phase separation of the polymers proceeds throughout the polymerization, which can result in other types of unique particle morphologies. Other heterogeneous

morphologies, such as hemispherical, particles with different types of inclusions, and "inverted" core-shell particles can occur depending on the various factors such as reaction conditions and the monomers selected. Synthesizing composite latex particles with well-defined morphologies is an important industrial process which also leads to many useful applications such as those found in coatings and adhesives.

A series of low T_g composite latexes with varying compositions were synthesized by seeded batch polymerizations and semi-continuous seeded polymerization methods. The core/shell weight % compositions of both series of latexes synthesized were 0/100, 25/75, 33/66, 50/50, 66/33 and 75/25. The seed (or core) latex consisted of poly(lauryl methacrylate) (PLMA), while the shell was a copolymer of poly(2-ethylhexyl methacrylate) (P2-EHMA) and 10 wt% benzyl methacrylate (BM) based on monomer. The benzyl methacrylate was added in order to be able to stain the latexes and differentiate the phases using transmission electron microscopy (TEM).

Different techniques may be applied in order to produce a core-shell particle structure by emulsion polymerization. Two different strategies were employed to synthesize core-shell morphologies using the PLMA/P2-EHMA system. The first strategy was the semi-continuous seeded emulsion polymerization technique. In this technique the second stage 2-EHMA monomer was fed semi-continuously into a reactor vessel containing PLMA seed polymer. Experimental results obtained in the literature have shown that homogeneous polymeric shells around polymeric seeds can be obtained using this technique by considering the following factors: (1) use of a water-soluble initiator, (2) adding monomer II under "monomer starved" conditions (3) higher water solubility of monomer II than that of monomer I can be helpful, but is not necessary (4)

incompatibility of the two polymers, which is almost always the case. [3] The experimental procedure used will be discussed in detail in the next chapter.

The second technique employed here to synthesize PLMA/P2-EHMA latex was a batch-type seeded (seed/swell) emulsion polymerization. The seed PLMA particles were first swollen by 2-EHMA monomer in sealed bottles for 24 hours at 23 °C while tumbling end-over-end in a tumbler. The exact experimental procedure used will be described in detail in the next chapter.

1.3 Latex Blends

Desirable mechanical properties in latex films can be achieved by synthesizing structured latex films such as the core-shell type. However, in many cases specific physical properties that are desirable in a latex film may be achieved by simply blending two or more different types of latexes. In this research project, differences in mechanical properties and morphologies of a composite latex system were investigated and compared to results obtained from latex blends of similar overall composition. The effect of crosslinking in one of the components in the blend, as well as in the composite latex system was investigated. Differences in the dispersion of the components in these systems after film formation is an important factor to be considered along with the extent of coalescence. Complete coalescence of latex particles with negligible voids is considered a characteristic of a good film having well-dispersed particles.[4] In addition, the amounts of each component in the system will also play an important role in this study. The mechanical behavior of the lower T_g polymer in a latex blend will generally

have a great effect on the strength of the latex film since it generally represents the continuous matrix. [5]

The core/shell weight % compositions of the latex blends were 0/100, 25/75, 33/66, 50/50, 66/33 and 75/25. More careful consideration was placed on the test results obtained from 33/66 wt% core/shell composite latexes and blends in each of the latex series that were synthesized. The 33/66 latexes had a higher modulus and more consistent results could be obtained from molded tensile specimens.

In addition, latex blending may be a viable strategy for removing organic solvent in coatings containing high T_g latex. In this case the organic solvent improves coalescence by swelling (softening) the polymer and lowering the T_g of the system. The alternative approach uses a dispersion of soft (low T_g) and hard (high T_g) polymers to replace the role of the organic solvent. In this manner, the low T_g particles may coalesce around the higher T_g particles to produce a composite-like effect. Studies showed that certain composition ratios of high to low T_g latex dispersions formed high quality, continuous films that were relatively hard, tough and durable. A synergistic effect was achieved in some cases, where the blend had better physical properties than the component homopolymers taken by themselves. [6]

1.4 Research Objectives

The research objectives for the study of low T_g PLMA/P2-EHMA-BM core-shell latexes are as follows:

1. Compare latex particle morphologies and mechanical properties of latexes prepared by seeded batch polymerization, semi-continuous polymerization and latex blends.
2. To correlate latex particle morphology, film formation and mechanical properties of the films.
3. Compare the effect of crosslinking in one of the phases and the effect of oil-soluble initiator 2,2'-azobis(isobutyronitrile) (AIBN) versus water-soluble initiator (potassium Persulfate) (KPS).

CHAPTER 2

EXPERIMENTAL

2.1 Materials

The LMA and 2-EHMA monomers were obtained from Sigma-Aldrich. The LMA and 2-EHMA monomers were cleaned before polymerization to remove inhibitor by passing them through an inhibitor-removal column (Sigma-Aldrich). The KPS (Aldrich), AIBN, and sodium bicarbonate (Aldrich) were used as received as the water soluble initiator, oil soluble initiator and buffer respectively. The surfactant used was Aerosol MA80 (Cytec Industries) which is composed of an 80% solution of sodium dihexyl sulfosuccinate in 5% isopropanol and 15% deionized (DI) water. Deionized water was used in all the experiments.

2.2 Preparation of Latexes

The PLMA seed latexes were prepared by a batch polymerization process using the recipe shown in Table 2-1. The recipe was developed in order to produce relatively narrow particle size distributions for the seed latexes.

Initially, polymerizations were carried out in 300 ml bottles. The surfactant and buffer were dissolved in 75 g DI water and then the lauryl methacrylate monomer was added into the bottle while stirring with a magnetic stirrer. The initiator was first dissolved in a separate beaker in the remaining DI water. All bottles and their contents were purged with nitrogen. The aqueous initiator solution was then added into the bottles. The bottles were sealed with a cap and a rubber gasket. They were then packed

in a cloth jacket and placed into the baskets in a bottle polymerizer. The bottles were rotated end-over-end at 40 rpm in a temperature-controlled water bath set at 70 °C for 18 hours.

Table 2-1: Typical Recipe for the Preparation of PLMA Seed and Composite Latexes

Seed Ingredients	**Amount (g)**	**Concentration**
Lauryl Methacrylate	24.31	
Aerosol MA80 (5 wt%)	52.00	43.7 mM[1]
Potassium Persulfate	0.104	2.5 mM[1]
Sodium Bicarbonate	0.0325	2.5 mM[1]
Deionized Water	104.00	
Shell Ingredients		≈25% solids overall
Poly (lauryl methacrylate)	100.0-150.0	
2-Ethylhexyl Methacrylate	7.4-48.6	
Benzyl Methacrylate	10.00 wt%[3]	
Potassium Persulfate or	0.028	1.0 mM[1]
2,2'-Azobis(isobutyronitrile)	0.0096	1.0 mM[2]

[1] based on aqueous phase
[2] based on oil phase
[3] based on 2-EHMA

Emulsion polymerizations of the PLMA seed were also carried out by conventional batch polymerization in a 500 ml round-bottom flask, equipped with a reflux condensor, at 70 °C for 6 hours using the same recipe as shown in Table 2-1. The polymerization was carried out in a nitrogen atmosphere. It should be noted that the shear produced in the bottle polymerizer during the reaction was different from the shear produced in the round bottom flasks using a Teflon paddle- type stirrer. The agitation speed was about 40 rpm.

The amounts of PLMA and 2-EHMA monomer used in the second stage polymerizations shown in Table 2-1 were varied in order to obtain a series of composite latexes with varying compositions.

For the semi-continuous seeded emulsion polymerizations a second stage shell was polymerized around the PLMA seed latex. The reactions were carried out in a 500 ml round bottom flask equipped with a reflux condensor, PTFE stirrer, nitrogen inlet tube and feeding tube for monomer. The PLMA seed and 10 wt% of the total second stage monomer mixture were placed into a sealed glass bottle inside a tumbler. The contents were tumbled end-over-end at room temperature for 2 hours in order to swell the latex. The contents of the bottle were bubbled with nitrogen gas and then put into the reactor at 75 °C. The remaining monomer mixture was fed into the reaction flask at a constant rate, approximately 0.14 ml/min. A Harvard syringe pump was used to feed the monomer into the flask at a steady rate. The polymerization was run for approximately 7 hours at 75 °C. The resulting latexes had solids contents ranging between 20 and 30% depending on the composition that was targeted for the particular composite latex. Different weight percent compositions of PLMA/2-EHMA-BM (33/66,50/50,66/33 and 75/25) were synthesized using this technique.

In addition, composite latexes of identical compositions were synthesized by a seed swelling (seed/swell) technique. The PLMA seed latex was swollen with the shell monomers for 24 hours at 23 °C while tumbling end-over-end in glass bottles. At the end of the tumbling cycle, KPS was added and then the bottles were purged with nitrogen gas and sealed. The polymerizations were carried out at 70 °C for 24 hours in a bottle polymerizer. Another series of latexes was synthesized by this technique using the same

ingredients except that 1 weight percent (based on monomer) of ethylene glycol dimethacrylate (EGDMA) crosslinker was added to the second stage monomers in order to crosslink this phase. A series of latexes were also synthesized according to the recipe in Table 2-1 using AIBN initiator instead of KPS.

2.3 Latex Characterization

The latex particle size distributions were measured using dynamic light scattering (Nicomp Model 370). Samples were diluted with DI water to obtain the optimal light scattering intensity value for the measurements as determined by the instrument (about 300 KHz). Particle sizes were also measured by capillary hydrodynamic fractionation (CHDF, Matec Applied Sciences, Model CHDF-1100). Samples for CHDF measurement were sonified in a sonifier bath to break up aggregates that may have formed. The final conversion of latexes were measured by gravimetry.

Glass transition temperatures (T_g) were measured by differential scanning calorimetry (DSC2920, TA Instruments). Samples for DSC measurement were taken from latex films and then dried in an oven at 75 °C for 3 days. Between 10 and 15 mg of dried latex was used and the tests were performed in nitrogen atmosphere at a flow rate of 50 cc/minute. A heating rate of 10 °C per minute was employed over a temperature range of –100 to +120 °C. Two temperature scans were performed on each sample and only the results of the second scan are reported here.

The mechanical properties of dried latex films were measured using an Instron universal tensile testing machine. Micro tensile specimens were prepared by compression molding at 100 °C for 25 minutes at a pressure of 2000 psi. The dimensions

for these specimens are specified in ASTM D638. A 500 N load cell was used, and the specimens were tested at 25 °C and a relative humidity of 50 %. Generally, between 3 and 5 specimens were used for each measurement and the results reported are the averages of those measurements.

Atomic force microscopy (AFM, Park Scientific,Topometrics) was used to study the surface morphology of dried latex samples. Samples were air dried at 23 °C on black-coated paper. The non-contact mode was used to obtain the AFM images.

CHAPTER 3

RESULTS AND DISCUSSION

3.1 The Critical Micelle Concentration (CMC) of Aerosol MA80 and Surface Tension Measurements

Aerosol MA80 (sodium dihexyl sulfosuccinate) is an anionic surfactant which was chosen since it is believed to aid in producing narrower latex particle size distributions. Narrow particle size distributions for the seed PLMA latexes were desirable in order to enable more effective analysis and comparisons of data. The HLB value of this surfactant is 12 indicating that it will work well in emulsion polymerization systems.[7]

It is important to avoid having excess surfactant left after polymerization of the seed in the second stage polymerization in order to avoid generation of new particles. Measuring surface tension will enable the determination of free surfactant in the aqueous phase in the latex after seeded emulsion polymerization. The surface tension versus Aerosol MA80 concentration is shown in Figure 3-1. The measurements were made using a bubble tensiometer (Sensadyne Corp.), at rate of 2 bubbles per second and a temperature of 29 °C.

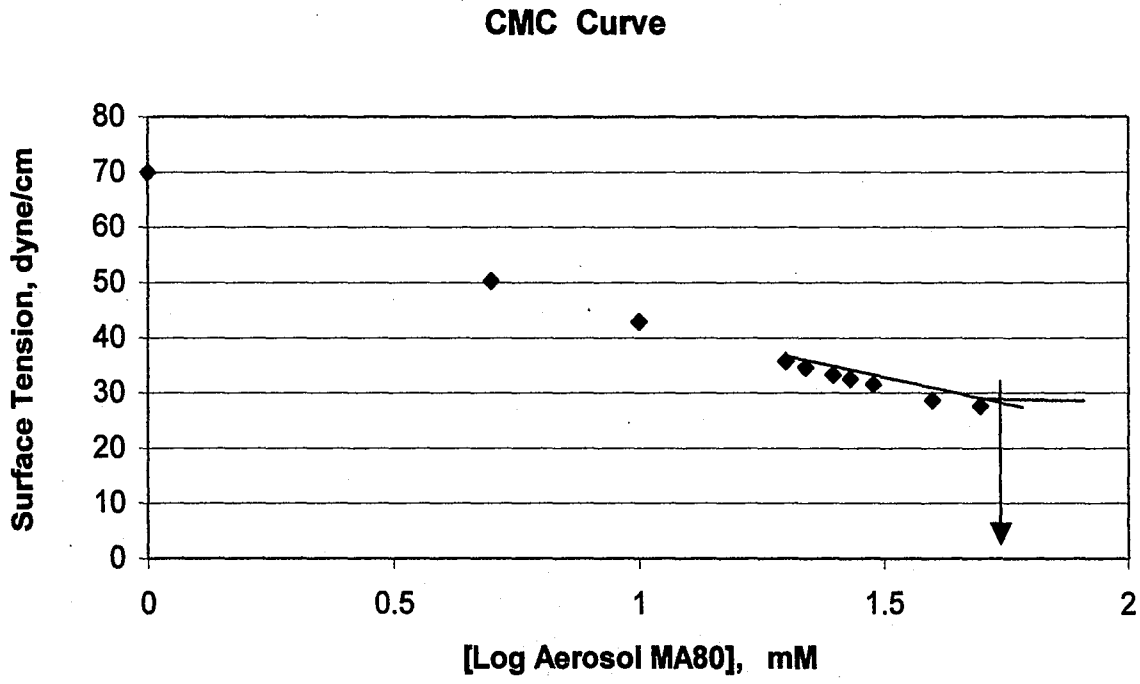

Figure 3-1: Surface tension versus Aerosol MA80 concentration in DI water at 29 °C showing a cmc value of 33 mM.

The cmc of Aerosol MA80 in DI water as determined by these measurements was 33 mM. The surface tension of the PLMA latex prepared by conventional batch emulsion polymerization was 30 dyne/cm which corresponds to 34 mM free surfactant in the aqueous phase. The adsorption area, A_s ,which is the area occupied by an emulsifier molecule at the polymer-water interface can be calculated. The adsorption area A_s calculated for this system based on a typical seed latex volume average diameter (D_v) of 87 nm was 162 A^2/molecule of surfactant.[8]

3.2 Lauryl Methacrylate and 2-Ethylhexyl Methacrylate Homopolymerizations

Initially, homopolymerizations of lauryl methacrylate (LMA) and 2-ethylhexyl methacrylate (2-EHMA) were carried out in order to develop a recipe for the PLMA seed and also to gain a better understanding of the behavior and properties of the monomers to be used in the synthesis of composite latex particles.

Measurements were made in order to determine the conversion-time curve of LMA. The typical recipe for synthesizing PLMA seed was outlined in Table 2-1. The experiment was carried out by bottle polymerization at 70 °C and samples were obtained at 8 different reaction times. Reactions were short stopped with 5 g of a 1% solution of hydroquinone at varying reaction times and the conversion was measured by gravimetry for each sample. Final particle size measurements were obtained using dynamic light

scattering (Nicomp Model 370) and the distributions are shown in Table 3-1. The weight average particle diameters (D_w), the volume average particle diameter (D_v) and the number average particle diameter (D_n) are shown in Table 3-1. Figure 3-2 shows the conversion-time curve obtained for the PLMA emulsion polymerization. The rate of polymerization (R_p) for PLMA was calculated to be approximately 1.25 x 10^{-4} moles/liter-sec. based on the initial linear portion of this curve. Some loss of monomer may have occurred since the final conversion obtained was 85%.

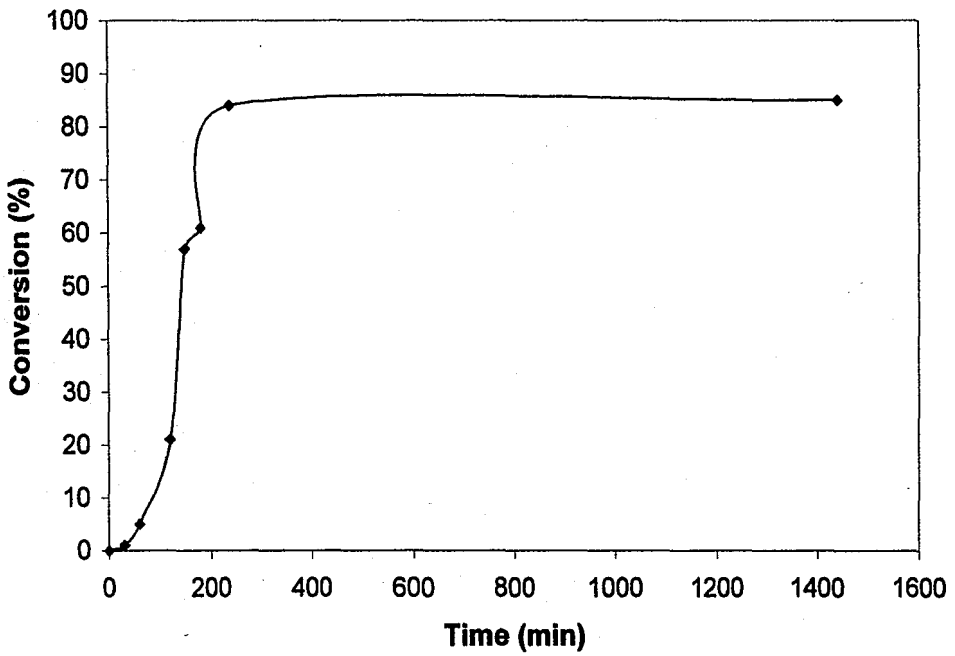

Figure 3-2: The conversion-time curve for LMA homopolymerization synthesized by batch emulsion polymerization at 70 °C using 2.5 mM KPS.

Homopolymerizations of 2-EHMA were also carried out using the same recipe used for the seed PLMA latex synthesis shown in table 2-1 except LMA is replaced by 2-EHMA monomer. The batch emulsion polymerizations were carried in bottles using a bottle polymerizer at 70 °C for 18 hours. The experimental preparation procedure was the same as that described in chapter 2 (section 2.2). Stable latexes were obtained with no coagulation present. Particle size results as measured by dynamic light scattering are shown in Table 3-1 along with conversion. The rate of polymerization for 2-EHMA under these conditions was estimated to be approximately 2.1 x 10^{-4} moles/liter-sec.

Table 3-1: Particle Size Distributions and Conversion for PLMA and P-2EHMA Homopolymers and P2-EHMA/BM Copolymer

Composition	D_w (nm)	D_v (nm)	D_n (nm)	PDI	Conversion %
PLMA homopolymer	89	87	85	1.05	85
P2-EHMA homopolymer	110	102	94	1.17	95
P2-EHMA/BM copolymer	106	97	88	1.20	95

3.3 Copolymer Synthesis

The shell polymer is a copolymer based on poly(2-ethylhexyl methacrylate-co-benzyl methacrylate) or P(2-EHMA/BM). A batch emulsion polymerization was carried out separately and the particle size results are shown in Table 3-1. A simple calculation using the Q-e scheme was made to determine the reactivity ratios for this system. The Q

and e values were found in the literature[9] and are shown together with the calculated values for r_1 and r_2 in Table 3-2.

Table 3-2: Q and e Values and Reactivity Ratios for P2-EHMA/BM Copolymer

Monomer	Q	e	Reactivity Ratios
2-EHMA	0.82	0.28	$r_1 = 0.95$
BM	0.88	0.35	$r_2 = 1.04$

Since both r_1 and r_2 are approximately equal to 1, the conditions are ideal and a random copolymer is expected. The copolymer should be of uniform composition.[9]

3.4 Characterization of Latexes by Particle Size Analysis and Conversion

The particle size and particle size distribution results of the semi-continuously polymerized composite latexes were obtained by dynamic light scattering (DLS) (Nicomp C370) and are shown in Table 3-3. The particle size data of the PLMA seed is also shown. These results show that high conversions were obtained for the seed latex as well as for the resulting composite latexes. The polydispersity indices (PDI) of the latex particle sizes remained relatively narrow (about 1.10 on average) throughout the experiments. There was little change in the PDI of the seed PLMA particles occurred in comparison to the final composite latex PDI values. No EGDMA crosslinker was used in this series.

Table 3-3: Particle Size, Particle Size Distribution and Conversion for the Semi-Continuously Polymerized Composite Latexes (DLS)

Composition PLMA/P2EHMA	D_w (nm)	D_v (nm)	D_n (nm)	D_v^* (nm)	PDI	Conversion %	N_p/L [b]
PLMA seed	103	99	94		1.09	98	2.79×10^{17}
75/25	136	127	122	109	1.11	95	
66/33	135	131	124	113	1.08	94	
33/66	173	167	154	143	1.12	96	
25/75	175	169	161	157	1.09	95	

* Expected D_v based on calculation

[b] Np/L is the number of particles per liter water

The number of particles, N_p , per liter of aqueous phase was calculated by:

$$N_p = \frac{6\,M}{\pi\,\rho_p\,D_v^3} \qquad (3.1)$$

where M [g/dm^3 H_2O] is the initial mass of monomer per volume of water, ρ_p [g/cc] is the density of the polymer, and Dv is the volume-average diameter of the latex particles (cm). The volume-average diameter of the PLMA seed was 99 nm. If one assumes that the number of particles N_p, before polymerization is the same as that obtained at the end of the second stage polymerization then the expected final latex particle diameter can be calculated. This would hold true as long as there is no second population of latex particles generated during the polymerization. This value is listed in Table 3-3 as D_v^*. The equation used to make this calculation was:

$$D_f^3 / D_s^3 = M_{fp} / M_{ip} \qquad (3.2)$$

Where D_f is the calculated final volume-average particle diameter of the composite latex (nm), D_s is the volume average diameter of the seed PLMA (nm), M_{fp} is the total final mass of polymer (g) and M_{ip} is the initial mass of seed polymer (g).

In all samples shown in Table 3-3, the calculated volume-average latex particle diameters are smaller than the measured values. It is suspected that some limited aggregation of the latex particles may have occurred, which would cause a larger particle size increase than expected. This could be due to a shortage of surfactant, since as the particle size increases, the system requires more surfactant to maintain colloidal stability. The particle sizes measured for the 33/66 and 25/75 showed very little change. This may have been due to latex particle aggregation.

Particle size distribution results obtained for the composite latexes synthesized by the seeded swelling emulsion polymerization technique were measured by DLS and are shown in Table 3-4.

Table 3-4: Final Latex Particle Distributions Measured by DLS for the Composite Core-Shell Latexes Prepared by the Seed/Swelling Method

Composition PLMA/P2EHMA	D_w (nm)	D_v (nm)	D_n (nm)	D_v* (nm)	PDI	Conversion %
25/75	317	321	306	278	1.04	94
33/66	251	239	229	252	1.09	95
50/50	208	135	128	200	1.09	94
66/33	197	192	183	159	1.08	94
75/25	196	190	182	150	1.08	93

*theoretical D_v

Table 3-5: Particle Size Distribution Results Measured By CHDF For the Composite Latexes Prepared by the Seed/Swelling Method

Composition PLMA/P2EHMA	D_w (nm)	D_v (nm)	D_n (nm)	D_v* (nm)	PDI	Conversion %
25/75	251	250	250	278	1.00	94
33/66	212	203	200	252	1.06	95
50/50	133	127	123	200	1.08	94
66/33	149	142	138	159	1.08	94
75/25	159	156	155	150	1.03	93

*theoretical D_v

Here again, the calculated volume average latex particle diameters were all smaller than the measured values except in the 33/66 case for the particles measured by light scattering. It is not clear why the 66/33 and 75/25 composites have larger particle diameters than the 50/50 particles. Perhaps some aggregation of these particles occurred to cause this increase. When the same latexes were measured using CHDF as shown in Table 3-5, the particle sizes obtained were all somewhat smaller as compared to light scattering results. Most of the average particle diameters obtained were smaller than the expected value for D_v except in the cases of the 75/25 and 50/50 ratio compositions. Figure 3-3 shows a typical CHDF result obtained for the particle size distribution of the 33/66 wt% core-shell latex synthesized by the seed/swell method. There was no large secondary population of particles detected here. The small bump in figure 3-3 at about

275 nm may be a small population of homopolymer latex from the second stage polymer or may be due to a small population of aggregated latex particles.

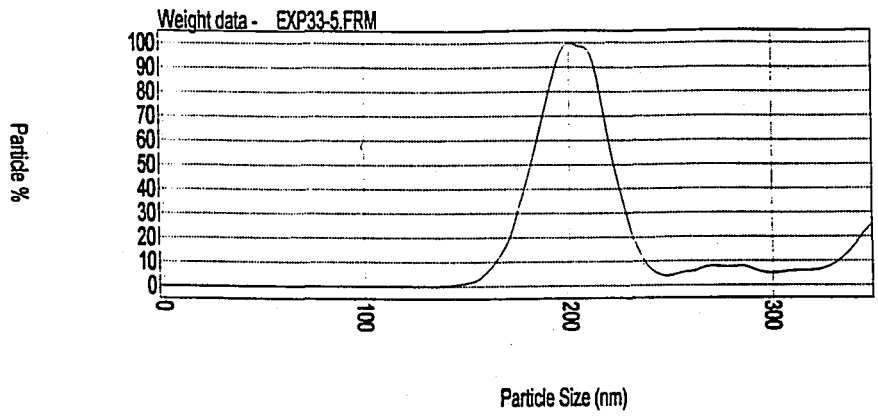

Figure 3-3: CHDF particle size distribution for D_w obtained for the 33/66 wt ratio core-shell latex synthesized by the seed/swell technique.

A series of composite latexes were also synthesized with 1 weight % EGDMA crosslinker added in order to crosslink the 2-EHMA phase in the composite system. Particle size analysis (DLS) for the composite latexes for this series is shown in Table 3-6. The final latex particle sizes measured were slightly larger than the calculated values in the case of the 25/75, 33/66 and 66/33 compositions. The 50/50 and 75/25 latexes were smaller than the theoretical values. It is possible that two particle size populations were generated, where one population has a smaller than expected particle size and the other population has a larger than expected particle diameter but smaller population. This can occur if enough surfactant was in the system to generate new particles composed of

the second stage monomers. Particle sizes of this series were also measured using CHDF. Results are shown in Table 3-7.

Table 3-6: Latex Particle Sizes of Composite Latexes with Crosslinked Shell (DLS)

Composition PLMA/P2EHMA	D_w (nm)	D_v (nm)	D_n (nm)	D_v* (nm)	PDI	Conversion %
PLMA Seed	85	83	80		1.07	93
25/75	139	136	133	131	1.05	94
33/66	131	128	126	119	1.04	94
50/50	112	102	91	104	1.22	95
66/33	101	99	95	96	1.06	95
75/25	100	97	94	91	1.06	93

*theoretical D_v

Table 3-7: Latex Particle Size Distributions for the Composite Core-Shell Latexes with Crosslinked Shells (CHDF)

Composition PLMA/P2EHMA	D_w (nm)	D_v (nm)	D_n (nm)	D_v* (nm)	PDI	Conversion %
PLMA Seed	85	83	81		1.07	93
25/75	136	134	133	131	1.02	94
33/66	130	127	126	119	1.03	94
50/50	129	109	103	104	1.25	95
66/33	99	95	93	96	1.06	95
75/25	109	107	106	91	1.03	93

*theoretical D_v

Results of particle size analysis by CHDF and DLS are in good agreement with one another. The largest difference in results between the two techniques was seen with

the 75/25 sample. Measurements by CHDF yield 107 nm for D_v and 97 nm by DLS. The 97 nm value (DLS) is closer to the theoretical particle diameter that was calculated. The data shows that the particles size distributions remained relatively narrow at the end of the second stage polymerizations with PDI values around 1.05 except for the 50/50 composite latex particles. The 50/50 composite latex had the broadest particle size distribution with a PDI value of 1.24. Similar to the results shown in Table 3-5, results given in Table 3-7 showed that the sizes obtained by CHDF were slightly smaller than the diameters measured by DLS. This was noticed here also except in the case of the 50/50 and 75/25 latexes.

It was decided to focus on the 33/66 wt% latexes since more consistent results in the mechanical properties test could be obtained. These results will be dealt with in chapter 3.6. Figure 3-4 shows a typical CHDF result obtained for the particle size distribution of the 33/66 wt% core-shell latex synthesized with EGDMA crosslinker. Only one single particle size population was detected.

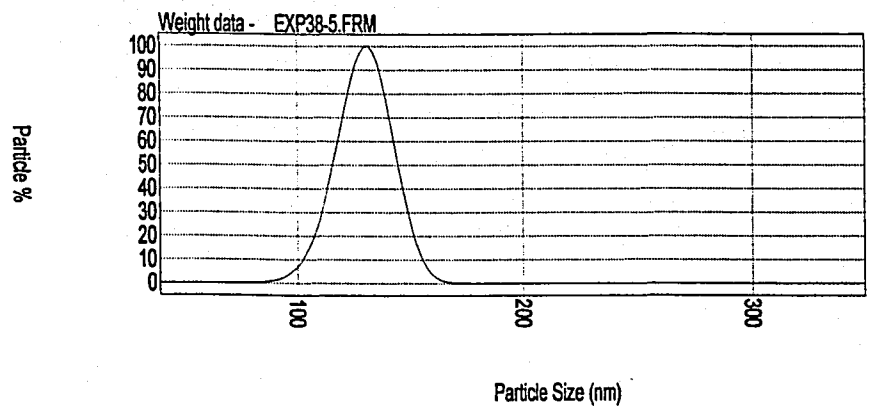

Figure 3-4: CHDF particle size distribution for D_w obtained for the 33/66 wt ratio core-shell latex synthesized with 1 wt% EGDMA crosslinker based on monomer.

A series of latexes were synthesized with 1 mM AIBN initiator in place of KPS in the second stage polymerizations for comparative studies. Particle size distribution were determined by DLS and CHDF, along with the conversion. The results are shown in Tables 3-8 and 3-9. The data shows that relatively high conversions were achieved similar to the previous series of latexes. It is not clear why the particles sizes measured by CHDF for the 75/25 latex was larger than that measured for the 66/33. Again, it is possible that some limited aggregation may have occurred. All of the measured particle sizes were slightly larger than the expected values as had been noted in the previous latex series.

Table 3-8: Latex Particle Size Distributions of Composite Latexes with AIBN Initiator (DLS)

Composition PLMA/P2EHMA	D_w (nm)	D_v (nm)	D_n (nm)	D_v* (nm)	PDI	Conversion %
PLMA Seed	85	83	81		1.07	93
25/75	159	155	149	131	1.07	94
33/66	152	148	142	119	1.07	93
50/50	124	121	118	104	1.05	93
66/33	115	111	109	96	1.06	93
75/25	108	108	108	91	1.00	94

*theoretical D_v

Table 3-9: Latex Particle Sizes of Composite Latexes with AIBN Initiator (CHDF)

Composition PLMA/P2EHMA	D_w (nm)	D_v (nm)	D_n (nm)	D_v* (nm)	PDI	Conversion %
PLMA Seed	85	83	81		1.07	93
25/75	160	143	131	131	1.22	94
33/66	131	125	121	119	1.08	93
50/50	121	118	117	104	1.03	93
66/33	112	107	103	96	1.09	93
75/25	136	112	108	91	1.26	94

*theoretical D_v

3.5 Glass Transition Measurements (T_g) by Differential Scanning Calorimetry (DSC)

For each sample of dried latex, two DSC scans were performed and only the results of the second scans were shown in order to remove the effects of thermal history. The glass transition values obtained for the composite latexes were compared to physical blends of similar composition of the respective homopolymer latexes. The software in the DSC instrument automatically calculates the T_g within a range that is selected by the operator. The inflection point method (I) for determining T_g was used to obtain all of the results reported here.

The T_g values for the homopolymers and copolymers along with the expected values obtained from the literature are shown in Table 3-10.[10] There are a couple of rea-

Table 3-10: Glass Transition Temperatures for The Copolymer and Homopolymers

Composition	T_g [Expected] (°C)	T_g [Measured] (°C)
PLMA	-65.0	-46.2
P2-EHMA	-10.0	-8.9
PBM	54.0	49.6
P2-EHMA -co- BM	-4.2*	-7.4

*calculated using the Fox equation.

sons why the measured T_g value for PLMA (- 46 °C) differs significantly from the literature value of - 65 °C. Slight crosslinking in the PLMA could raise its T_g, however, this reason is less likely since low degrees of crosslinking should only increase the T_g a few degrees, not 19 °C as is exhibited here. More likely, the differences between these

two values lies in differences in the number-average molecular weight (M_n) of the PLMA sample tested in the literature and the samples prepared here for this study. The T_g of our samples probably had a higher M_n than the sample tested in the literature, since T_g will increase with M_n. The glass transition increases with M_n to a limiting asymptotic value of T_{g0} for infinite molecular weight, where $T_g = T_{g0} - 1.8 \times 10^5/M_n$. In addition, differences in the heating rates could also lead to values that deviate from the literature. The other T_g values reported in Table 3-10 are within experimental error (+/-4 °C) . It is expected that slight crosslinking is more likely to occur in the P2EHMA/PBM domains than in PLMA. This may be due to double bonds found in BM.[11]

Table 3-11 shows the typical T_g values measured for the composite latexes synthesized without crosslinker along with the T_g results of the simple blends of the PLMA homopolymer and P2EHMA -co- BM copolymer. In general, the T_g values for

Table 3-11: Glass Transition Measurement Results For the PLMA/P2-EHMA -co- BM Composite Films and Latex Blends

Composite Latexes	**T_{g1} [PLMA] (°C)**	**T_{g2} [P2-EHMA/BM] (°C)**	**T_{g3} [P2-EHMA/BM] (°C)**
25/75 composite	- 43.2	- 9.2	
33/66 composite	- 48.5	- 15.6	10.9
50/50 composite	- 48.4	- 11.0	
66/33 composite	- 44.0	- 7.0	
75/25 composite	- 46.5	- 7.0	
Latex Blends			
25/75 Blend	- 42.6	- 10.2	
33/66 Blend	- 43.4	- 13.1	4.7
50/50 Blend	- 41.0	- 9.0	13.6
66/33 Blend	- 43.0	- 11.0	
75/25 Blend	- 45.6	- 11.1	

the PLMA portions in the latex blends and composites are only slightly higher than the T_g of the PLMA homopolymer. This means that there is only very slight miscibility between the two phases. The T_gs for the copolymer phase in the latex blends are only slightly lower than the pure copolymer T_g value of – 8.9 °C; again, this indicates only slight miscibility. True core-shell polymer would exhibit two well-defined transitions as indicated for the composite latexes. In some cases a weak third transition appeared in the DSC which is recorded in column 3 of Table 3-11. This transition could be due to noise and is considered an artifact.

Figure 3-5(a)-(d) shows some typical DSC results obtained for the composite latex particles and latex blends. Figures 3-5(a) and (b) show typical results obtained for the 33/66 composite latex (seed/swelling) and latex blend. Figures 3-5 (c) and (d) show all results for the entire series of composite latexes and latex blends over-layed on top of each other. Some noise is evident in the 25/75 composite around 0 °C.

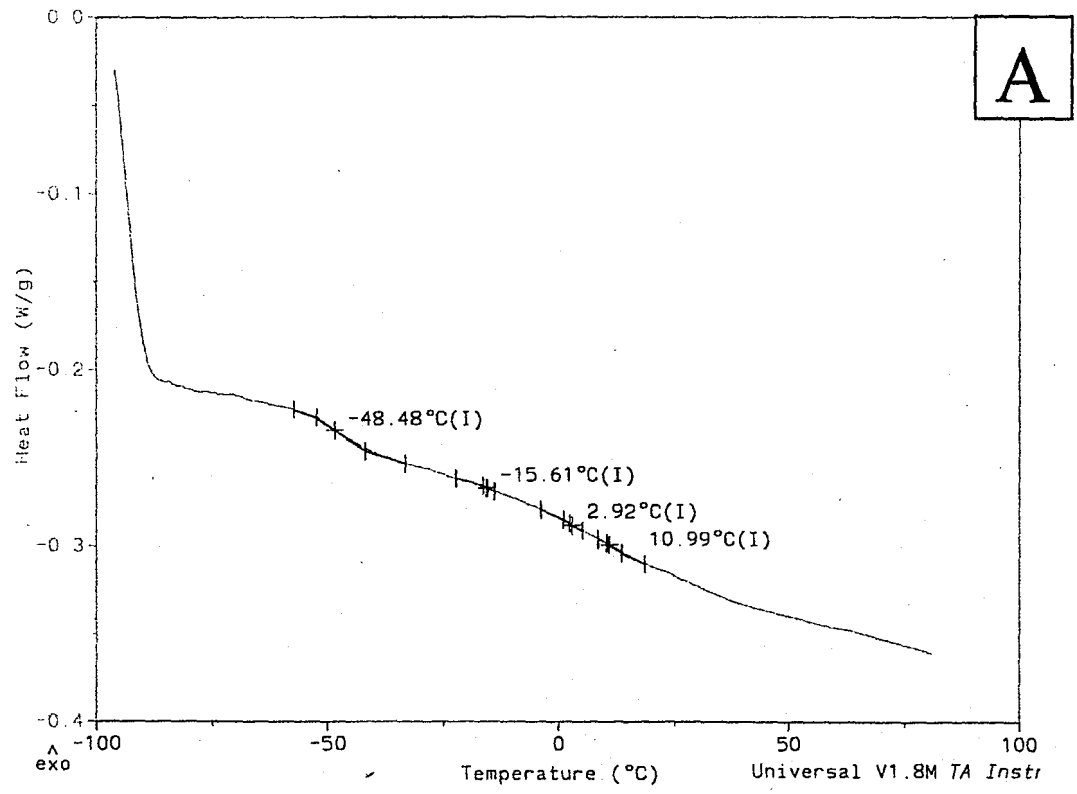
A
0.0
-0.1
-0.2
-0.3
-0.4
Heat Flow (W/g)
-48.48°C(I)
-15.61°C(I)
2.92°C(I)
10.99°C(I)
-100
-50
0
50
100
exo
Temperature (°C)
Universal V1.8M TA Instr

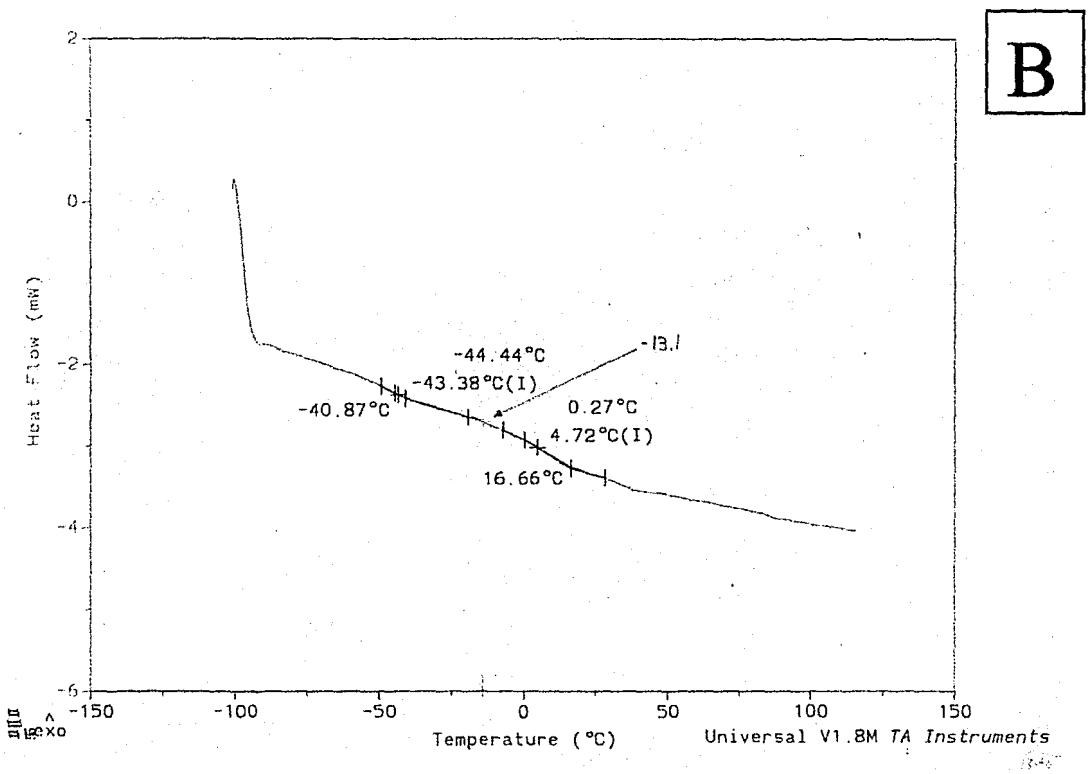
B
2
0
-2
-4
-6
Heat Flow (mW)
-44.44°C
-43.38°C(I)
-40.87°C
0.27°C
4.72°C(I)
16.66°C
-150
-100
-50
0
50
100
150
exo
Temperature (°C)
Universal V1.8M TA Instruments

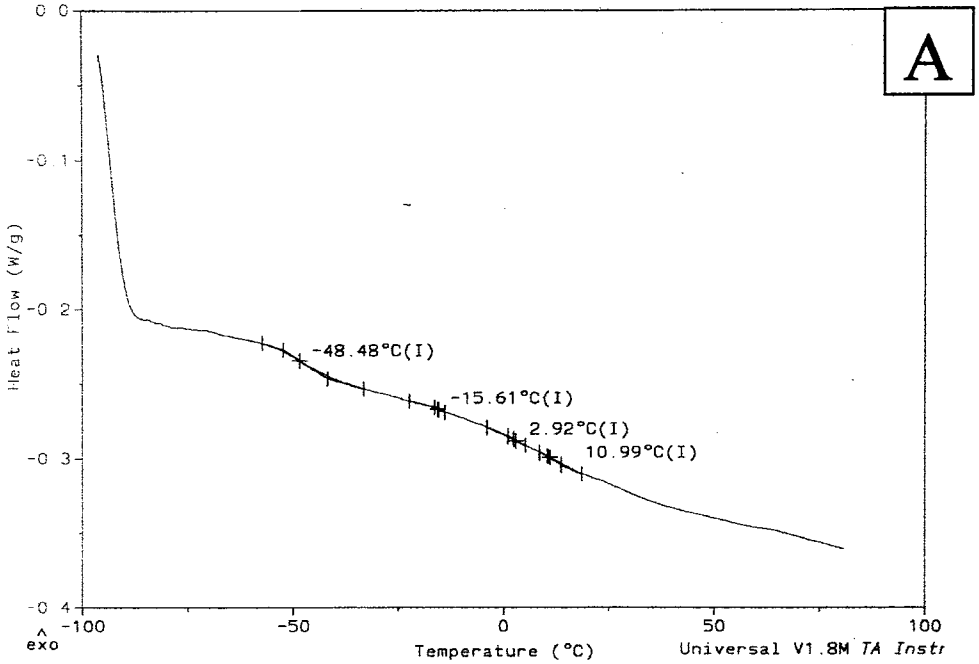

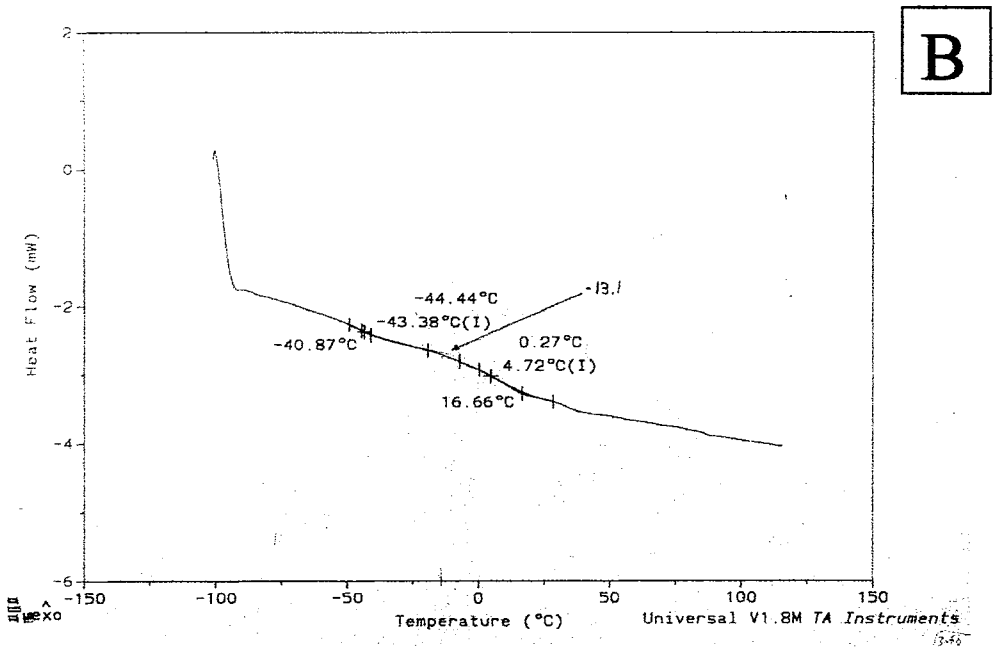

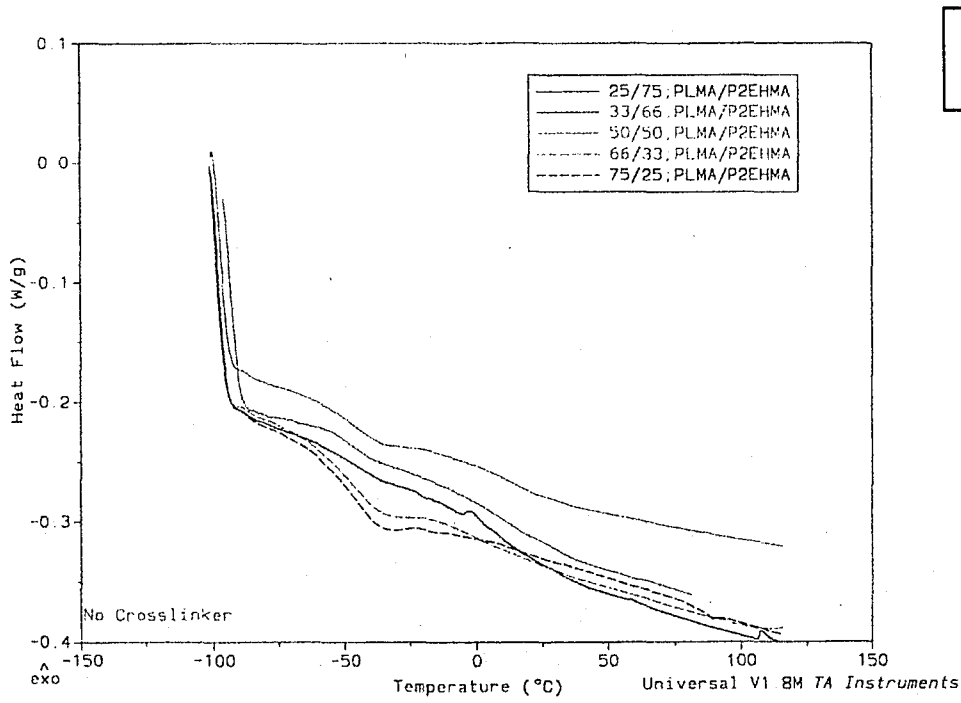

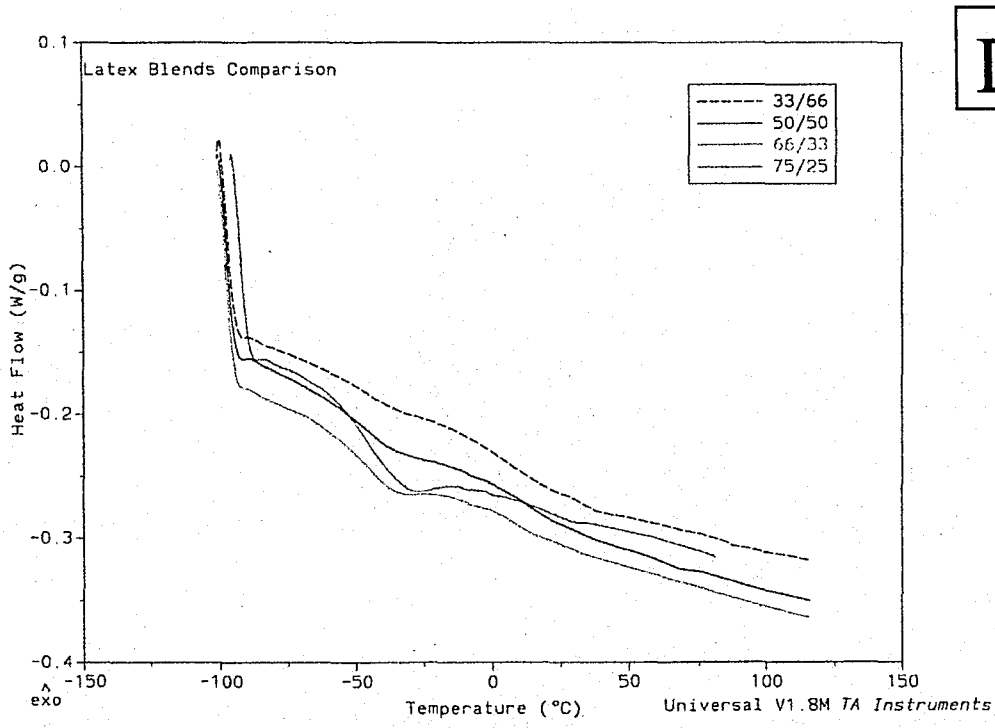

Figure 3-5(a): DSC results of PMMA/P2EHMA (33/66) dried latex film synthesized using a seed/swell polymerization; **(b)** results for the PMMA/P2EHMA (33/66) latex blend; **(c)** results for the series of PMMA/P2EHMA latexes of different wt% compositions and the corresponding physical blends without crosslinker **(d).**

C

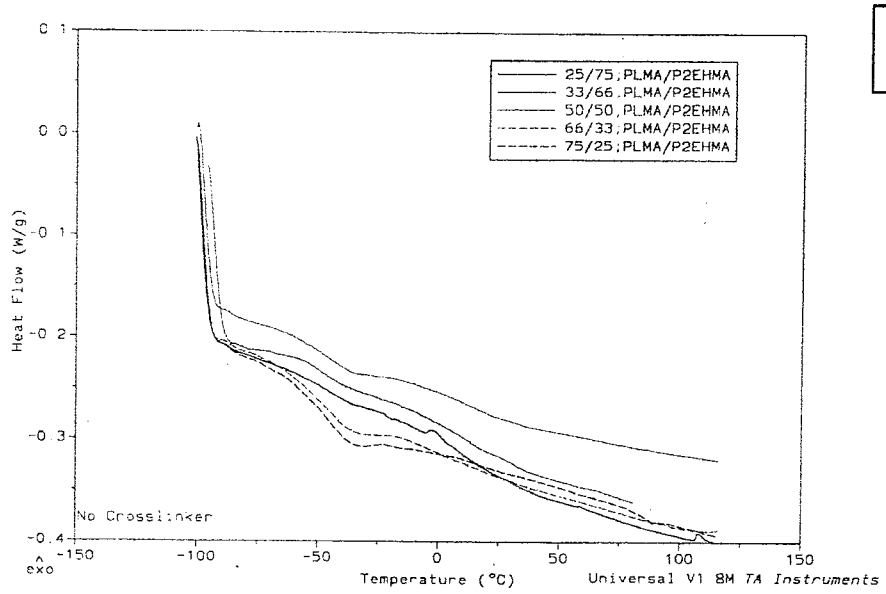

D

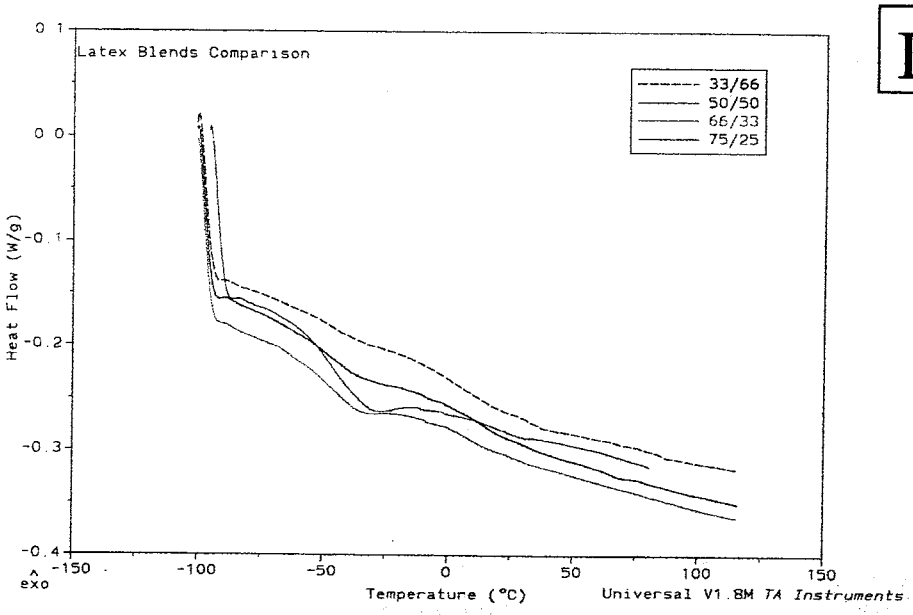

Figure 3-5(a): DSC results of PMMA/P2EHMA (33/66) dried latex film synthesized using a seed/swell polymerization; **(b)** results for the PMMA/P2EHMA (33/66) latex blend; **(c)** results for the series of PMMA/P2EHMA latexes of different wt% compositions and the corresponding physical blends without crosslinker **(d).**

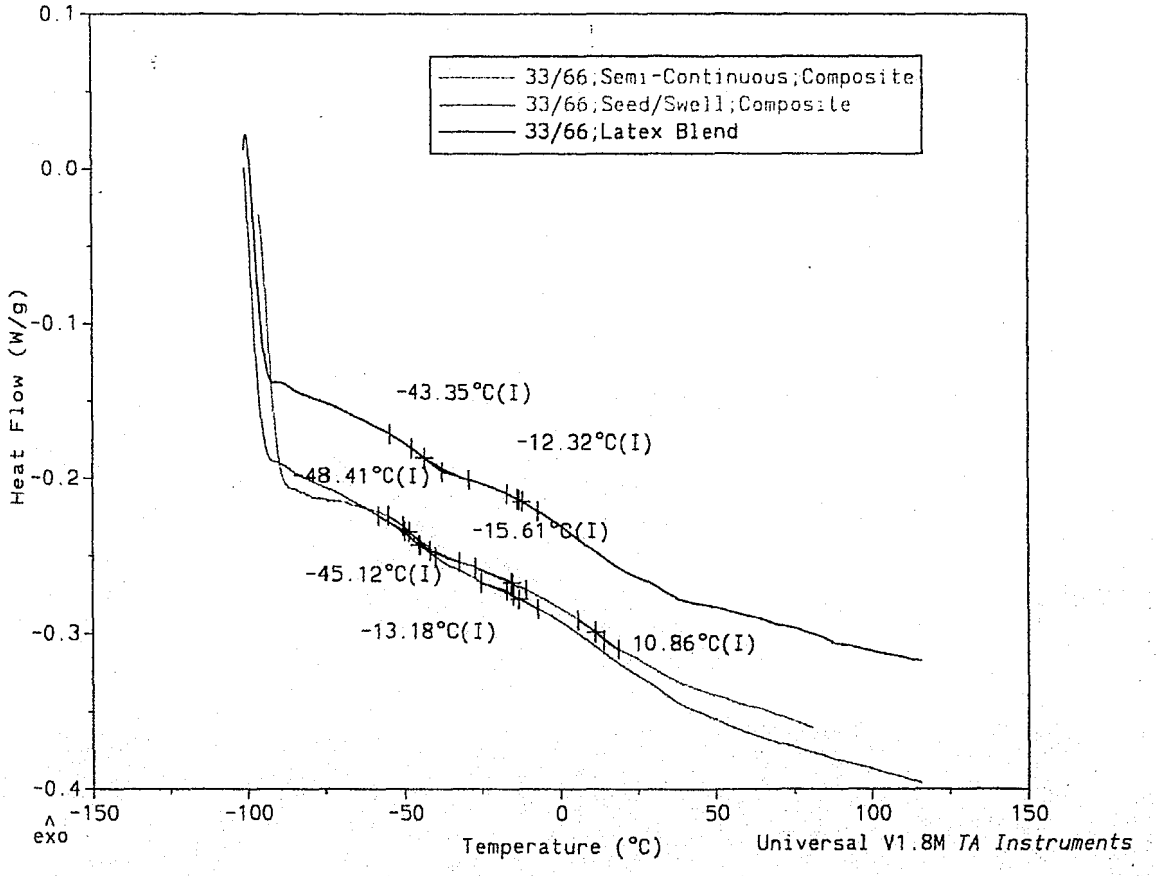

Figure 3-6: DSC results of PLMA/P2EHMA results of the seed/swell latexes compared to semi-continuous polymerization results and physical blend.

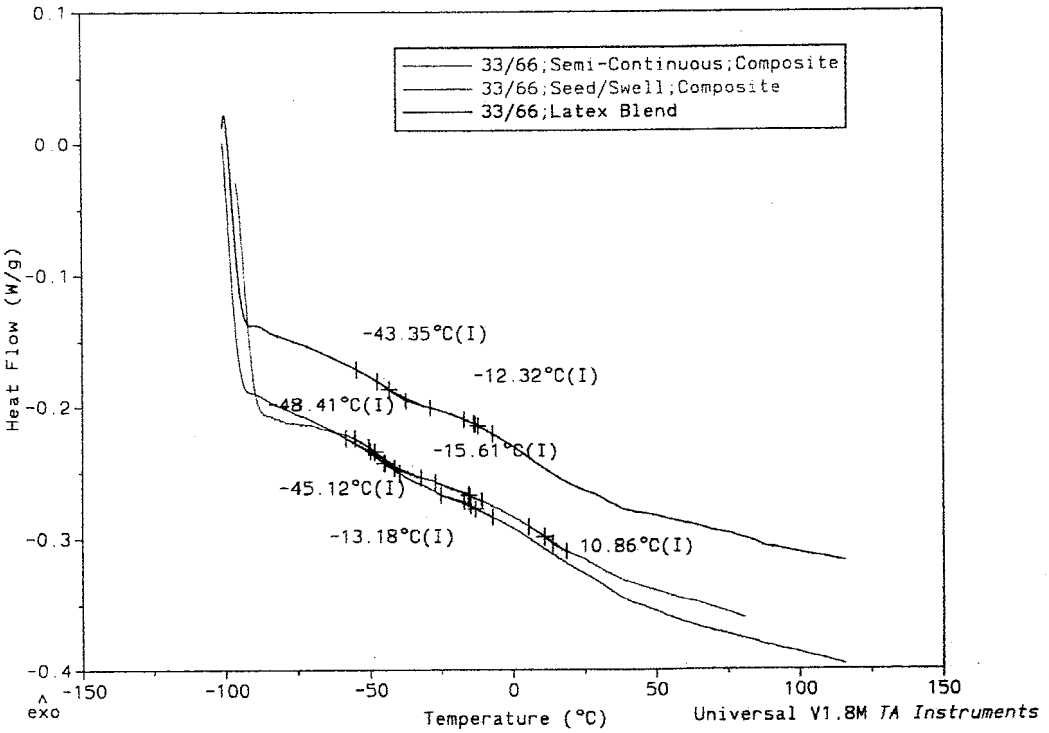

Figure 3-6: DSC results of PLMA/P2EHMA results of the seed/swell latexes compared to semi-continuous polymerization results and physical blend.

Figure 3-6 shows a comparison of the T_g values obtained from the PLMA/P2EHMA (33/66) seed/swell composite latexes compared to those synthesized by a semi-continuous process and a simple physical blend. On a qualitative basis, the glass transitions obtained from the semi-continuous process appear to be broader and not as well defined as compared to the seed/swell process and especially the physical blend. This may indicate that greater miscibility between the two phases is achieved in the semi-continuous process.[12] The transition shown at 10.9 and 32 °C in this figure is most likely an artifact due to instrument noise. The T_gs of the PLMA in the seed/swell and semi-continuous films seem to be within experimental error of one another at – 48 and – 45 °C respectively, whereas the T_g of the PLMA domains in the latex blend (- 43 °C) is the furthest from the measured T_g value of PLMA homopolymer (-46 °C).

Table 3-12 shows the DSC results obtained for the composite latex particles synthesized by the seed/swelling method using 1 wt % EGDMA crosslinker in order to crosslink the P2EHMA domains.

Table 3-12: DSC Results For the PLMA/P2-EHMA-co-BM Composite Films Synthesized With EGDMA Crosslinker

Composite Latexes	**T_{g1} [PLMA] (°C)**	**T_{g2} [P2-EHMA/BM]**	**T_{g3} [P2-EHMA/BM]**
25/75 composite	- 45.6	11.1	33
33/66 composite	- 46.2	- 0.80	38.2, 53.4
50/50 composite	- 43.9	- 4.3	49.6
66/33 composite	- 46.0	- 3.1	- 10.9, 4.8
75/25 composite	- 42.8	- 1.9	

The T_g values for the PLMA domains in the composite latexes shown in Table 3-12 (T_g1 column) are within the expected values for PLMA homopolymer. However, it can be seen that in all cases the T_gs for the P2EHMA/BM domains (T_g2 column) all increased several degrees in comparison to the values obtained in Table 3-11 for the series with no crosslinker. This shows that the EGDMA crosslinker produced a lightly crosslinked network in the P2EHMA/BM domains. Additional weak transitions that were seen in these DSC scans are tabulated in the T_g3 column of Table 3-12. Some of these values may have real significance and others may simply be artifacts. For instance the values of 53.4 °C and 49.6 °C for the 33/66 and 50/50 composites, respectively, fall at the value expected for BM homopolymer. Perhaps, a very small amount of a second population of BM homopolymer may have been generated in some of these latexes. However this second population was not seen in the analysis of the particle size distributions. In the 66/33 DSC scan, different transitions were detected. Perhaps, some non-uniform crosslinking may have occurred which would cause some particles to be more crosslinked than others. This could cause different T_g values to ocurr within a few degrees of one another as was seen in the 66/33 latex T_gs. The values of – 10.9, - 3.1 and 4.8 °C were measured. Figure 3-7 shows the complete results of DSC analysis overlayed on top of each other for the PLMA/P2EHMA series with crosslinker present.

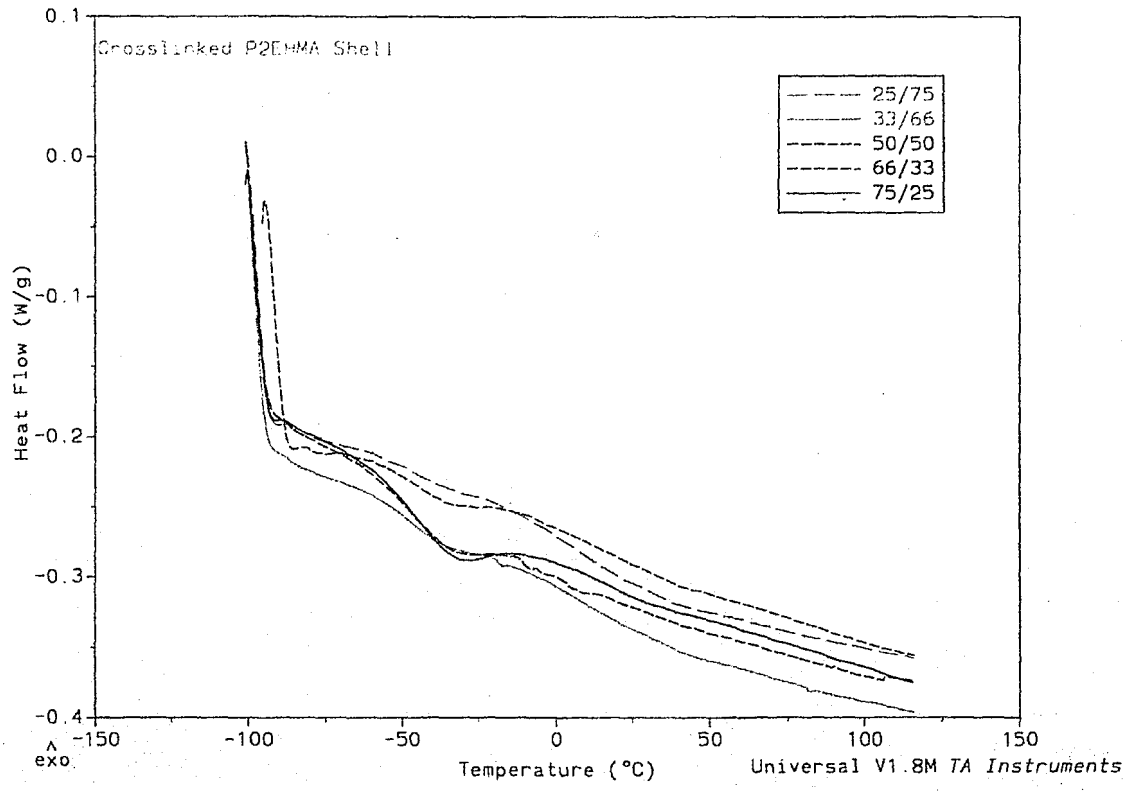

Figure 3-7: DSC results for the series of PMMA/P2EHMA latexes of different wt% compositions with crosslinker.

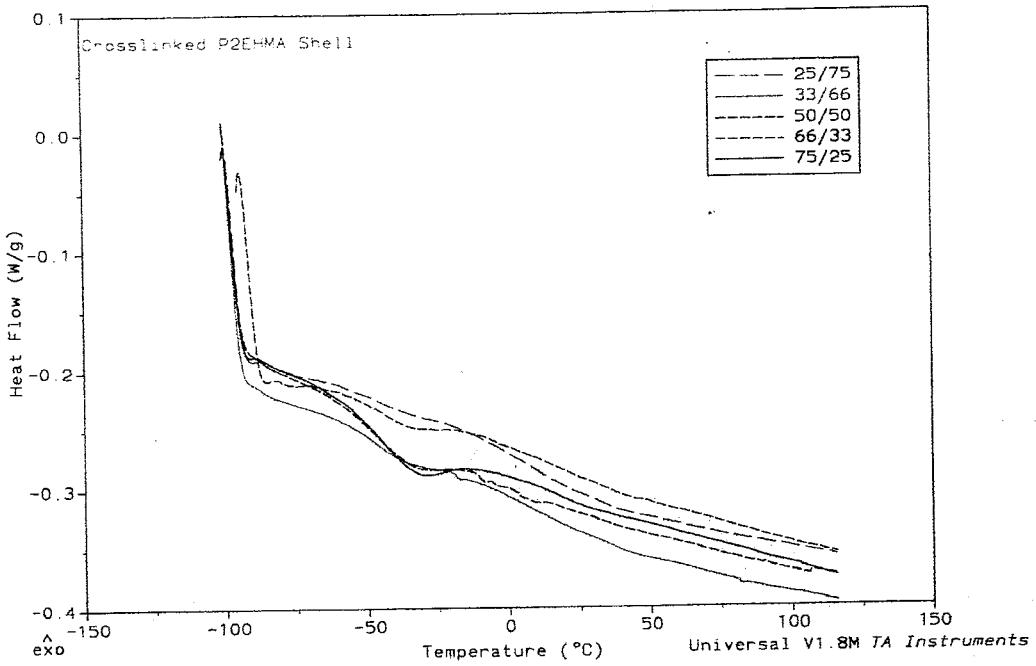

Figure 3-7: DSC results for the series of PMMA/P2EHMA latexes of different wt% compositions with crosslinker.

Table 3-13 shows the DSC results obtained for the composite latex particles synthesized by the seed/swelling method at 70 °C using 1 mM AIBN initiator instead of KPS.

Table 3-13: Thermal Characteristic Results For the PLMA/P2-EHMA-co-BM Composite Films and Latex Blends Synthesized with AIBN Initiator

Composite Latexes	**T_{g1} [PLMA] (°C)**	**T_{g2} [P2-EHMA/BM] (°C)**	**T_{g3} [P2-EHMA/BM] (°C) Artifacts**
25/75 composite	- 40.9	- 4.0	6.3
33/66 composite	- 46.0	- 7.5	
50/50 composite	- 41.4	- 11.0	17.2
66/33 composite	- 48.3	- 2.0	13.6
75/25 composite	- 48.0	- 0.82	

The T_gs as shown in Table 3-13 are similar to those presented in Tables 3-11 and 3-12. The variations that are seen in the T_{g1} and T_{g2} values may also be due to variations in the amount of crosslinking from series to series. Figure 3-8 shows the complete results of DSC analysis overlayed on top of each other for the PLMA/P2EHMA series with AIBN as initiator. The T_gs for the P2-EHMA/BM phases shown in Table 3-13 appear to have increased overall in comparison to the results obtained for the series using KPS initiator (Table 3-11). However, the T_gs for the PLMA phases shown in Table3-13 remained relatively unchanged in comparison to the series using KPS initiator.

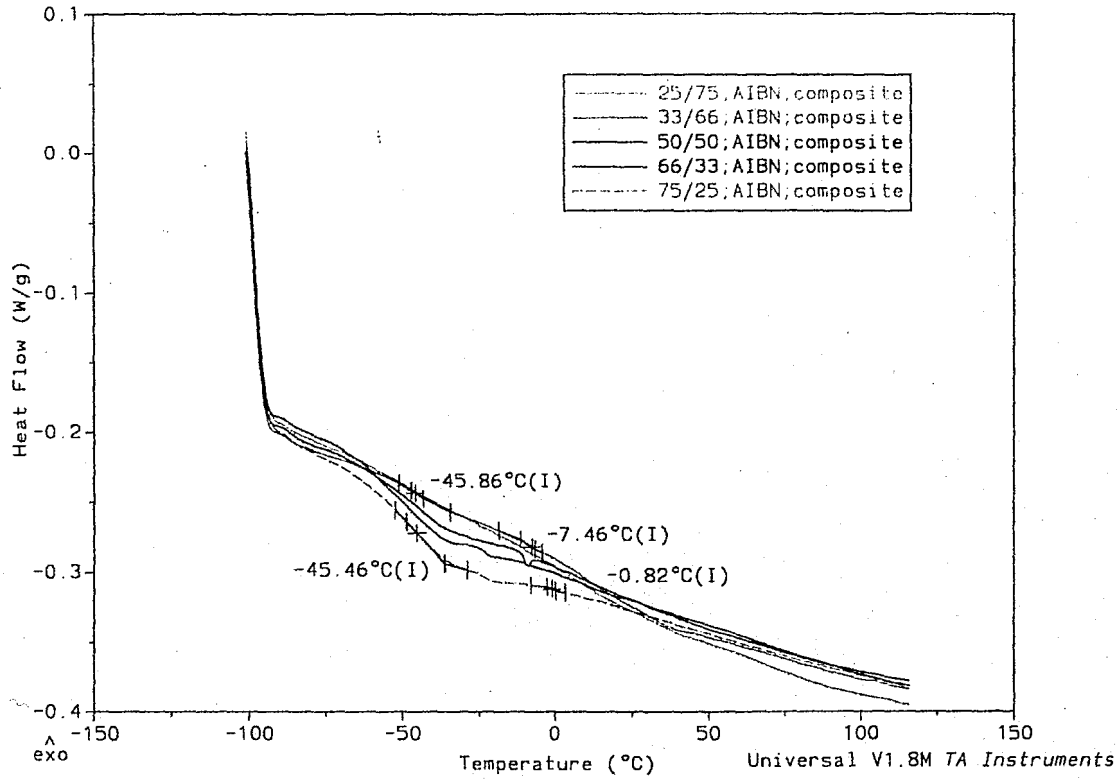

Figure 3-8: DSC results for the series of PMMA/P2EHMA latexes of different wt% compositions with AIBN initiator

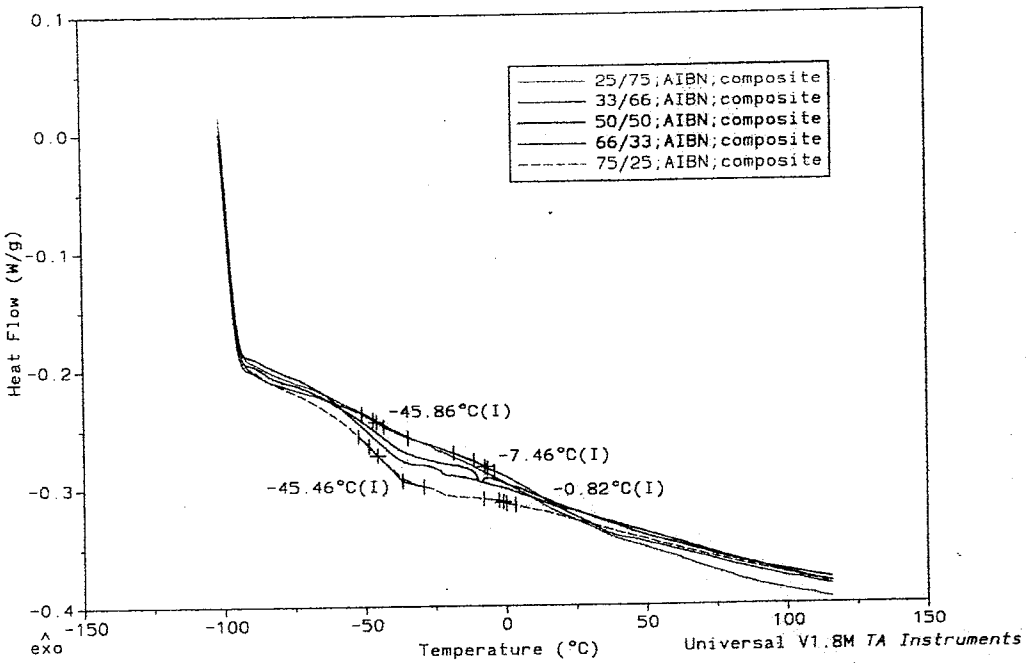

Figure 3-8: DSC results for the series of PMMA/P2EHMA latexes of different wt% compositions with AIBN initiator

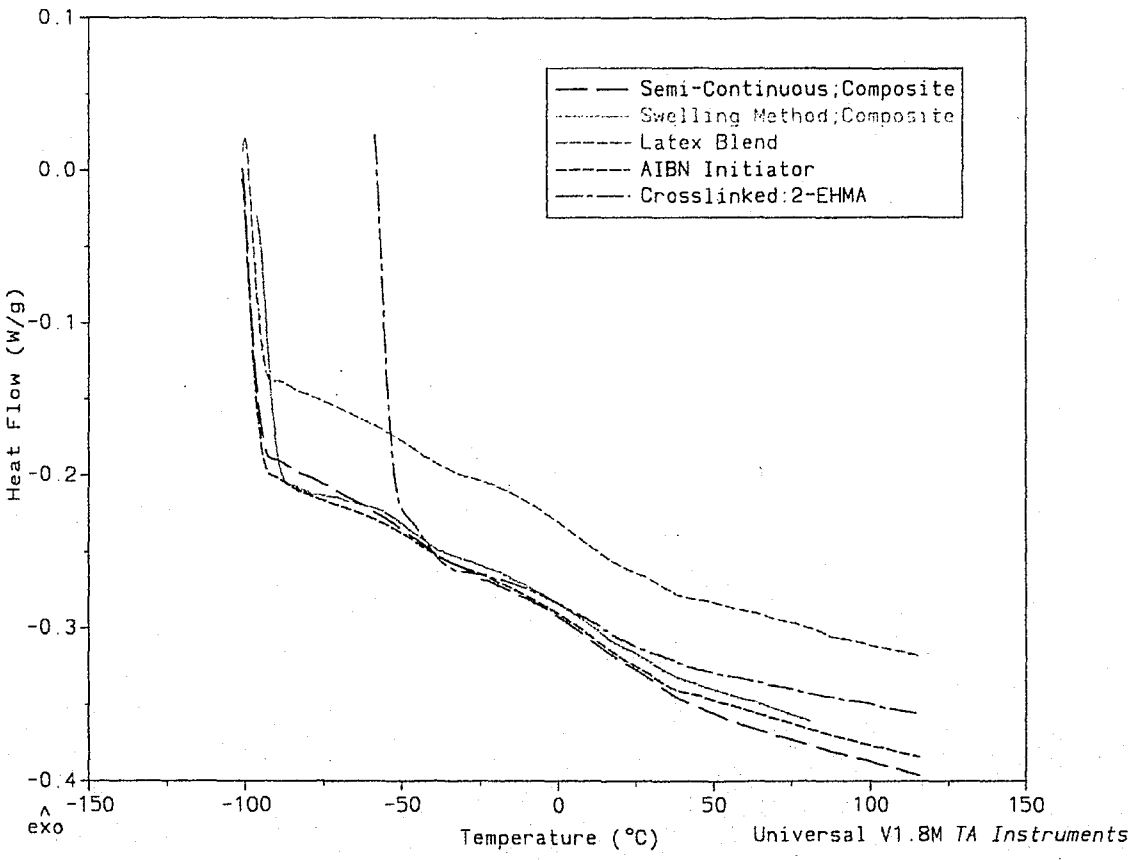

Figure 3-9: DSC comparison for the series of (33/66) PMMA/P2EHMA latexes with varying synthesis techniques

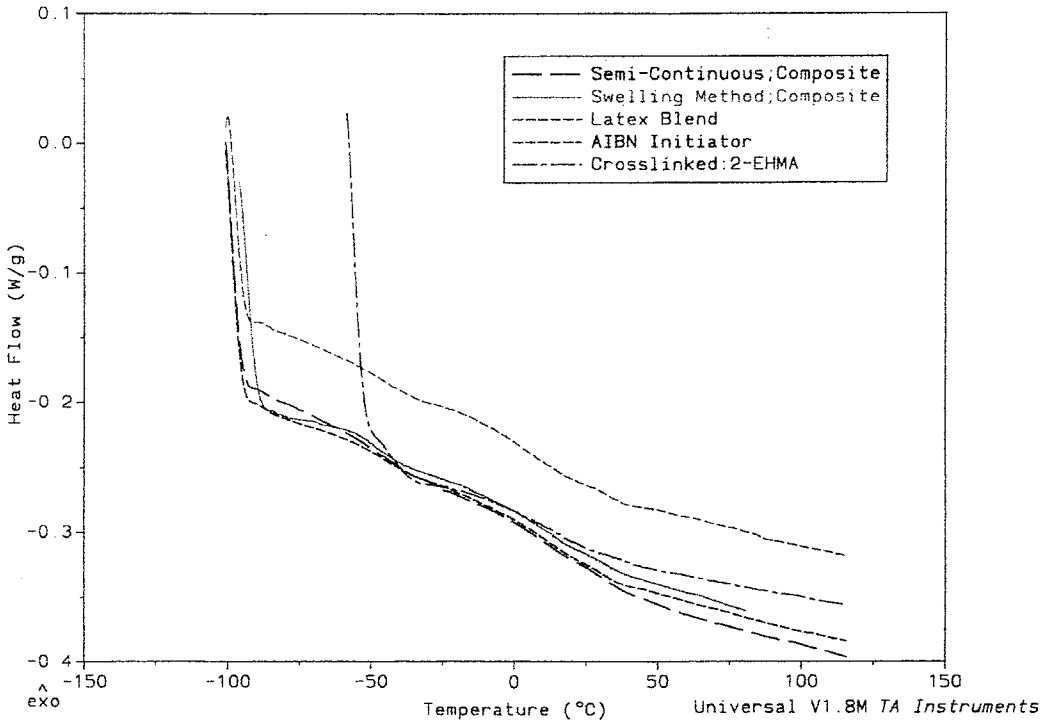

Figure 3-9: DSC comparison for the series of (33/66) PMMA/P2EHMA latexes with varying synthesis techniques

3.6 Mechanical Properties Characterization of Latex Films

The mechanical properties of the dried latex films were measured using an Instron tensile testing machine. Table 3-14 is a summary of the data collected for the dried composite latex films with no added crosslinker versus physical blends of similar composition. The corresponding composition versus toughness and elongation curves are shown in Figures 3-10 through 3-12. The toughness is automatically calculated by the instron software and is the area under the stress-strain curve. Latex blends of similar compositions were tested for comparative studies.

Table 3-14: Stress-Strain Properties of Composite Latexes versus Latex Blends of Similar Composition

Sample PLMA/P2EHMA	Stress at break (MPa)	% Strain at break (MPa)	Modulus (MPa)	Toughness (MPa)	Maximum Strain (mm/mm)
Composite latexes					
0/100	2.27	947.00	7.91	16.24	9.78
25/75	2.70	1272.00	5.97	21.60	14.20
33/66	1.80	1370.03	3.97	16.60	13.70
50/50	0.58	608.00	2.32	3.12	6.10
66/33	0.59	1319.04	0.93	5.80	13.62
75/25	0.49	1973.00	0.38	8.50	20.67
Latex blends					
0/100	2.27	947.03	7.91	16.24	9.78
25/75	1.99	1089.00	7.79	15.35	10.90
33/66	0.49	920.00	2.61	11.20	9.30
50/50	1.00	855.00	4.02	7.03	8.58
66/33	0.69	1476.01	0.50	6.07	14.79
75/25	0.50	2010.00	0.40	8.30	19.00

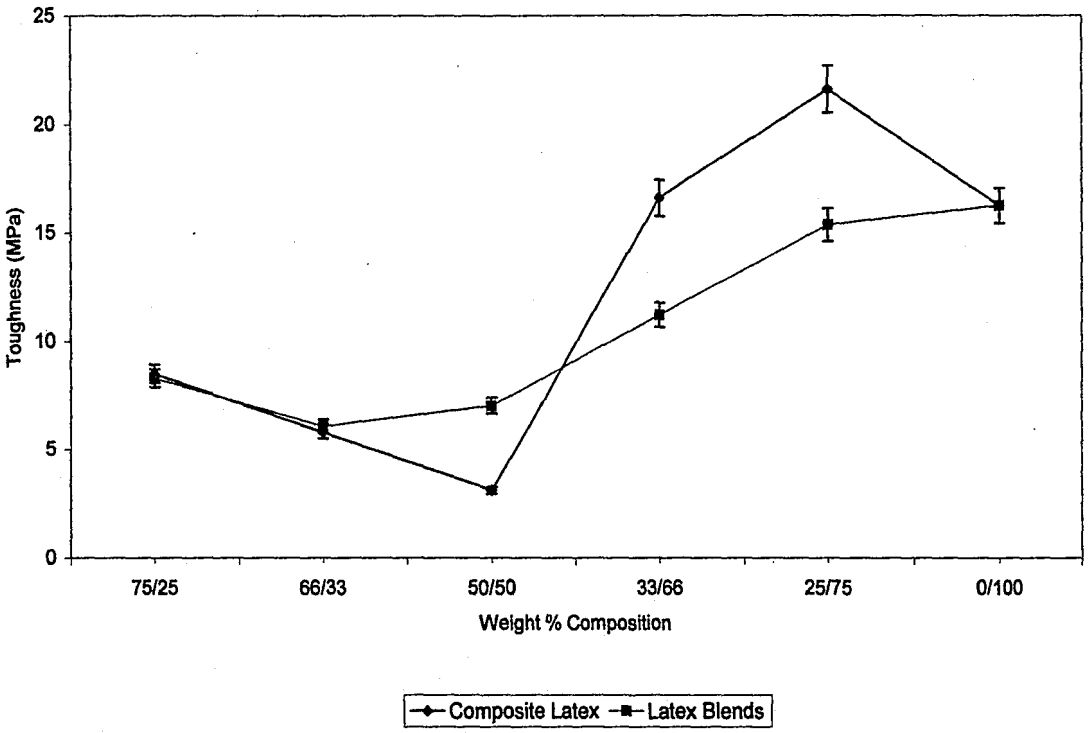

Figure 3-10: Toughness versus composition of micro tensile specimens of composite PLMA/P2EHMA latexes and latex blends with no crosslinker present.

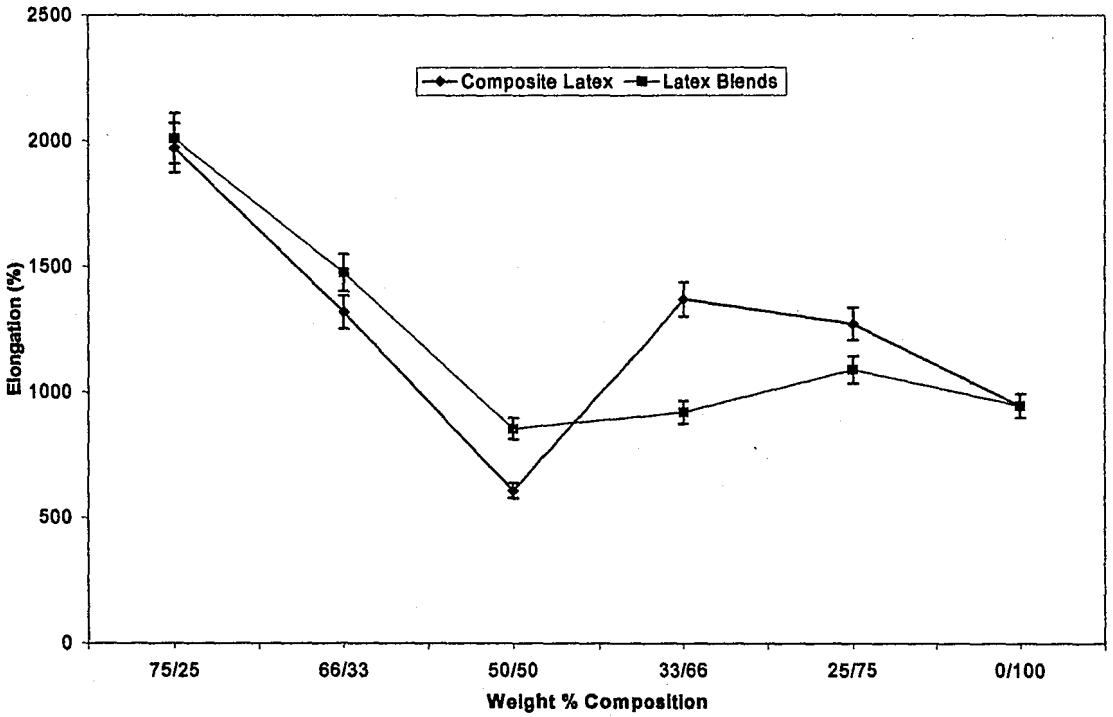

Figure 3-11: Elongation versus composition of composite PLMA/P2EHMA latexes and latex blends with no crosslinker.

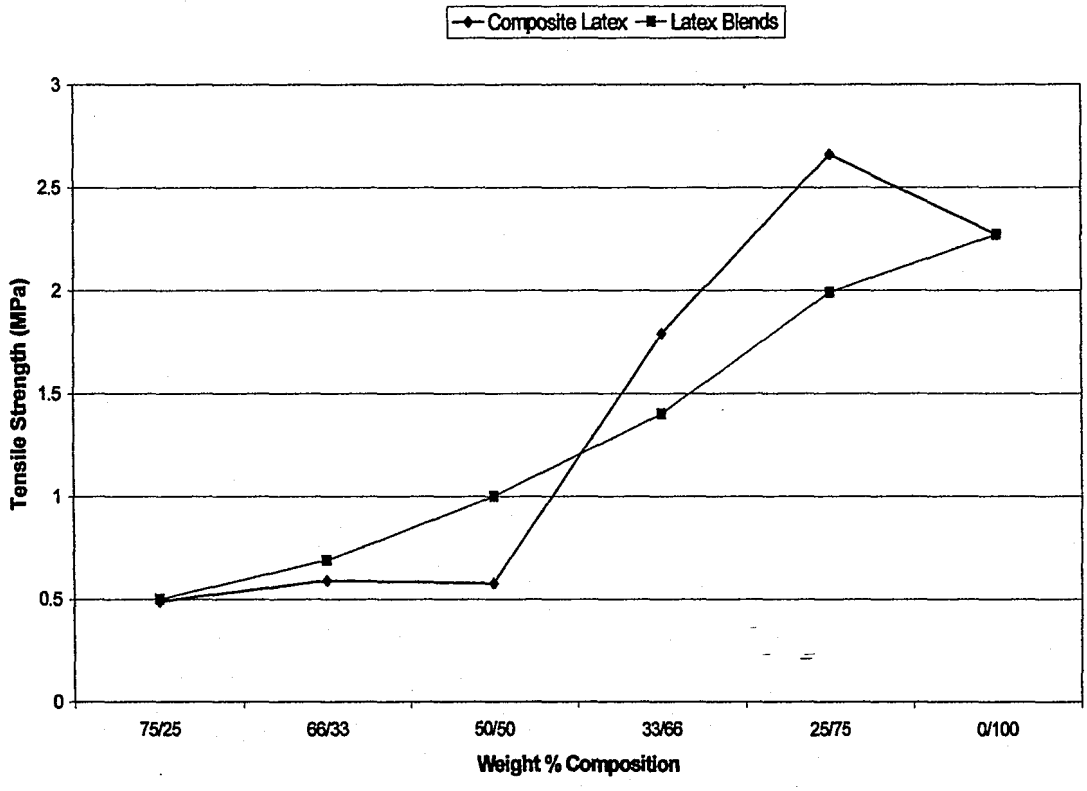

Figure 3-12: Tensile strength versus composition of micro tensile specimens of composite PLMA/P2EHMA latexes and latex blends with no crosslinker present.

The mechanical properties of both latex blends and composites were very similar for the 75/25 and 66/33 weight percent PLMA/P2EHMA compositions. As the composition was varied from 66/33 to 50/50, a transition point seems to have occurred where the mechanical properties of the composites were higher than those of the blends. Only in the case of the 50/50 composition was there a gradual increase in the mechanical properties of the latex blend compared to the composite. Moving from the 50/50 composition to the 33/66 and 25/75 compositions, the mechanical properties of the composites were higher than the blends. The mechanical properties of the composites for the 33/66 and 25/75 latexes showed an increase in toughness, tensile strength and elongation in comparison to the latex blends. It is expected that there is no significant crosslinking in either the latex blends or core-shell latexes in this series. If there were larger amounts of crosslinking in one system then this could result in the higher mechanical properties measured. Perhaps, the composite latexes had more uniform dispersion of the phases throughout the films than the films from the latex blends. This point will be discussed further in the section describing the results of AFM studies on these films (section 3-7). The 100/0 weight percent composition data point was not obtained due to its extreme rubbery and soft nature. It was not possible to compression mold this film.

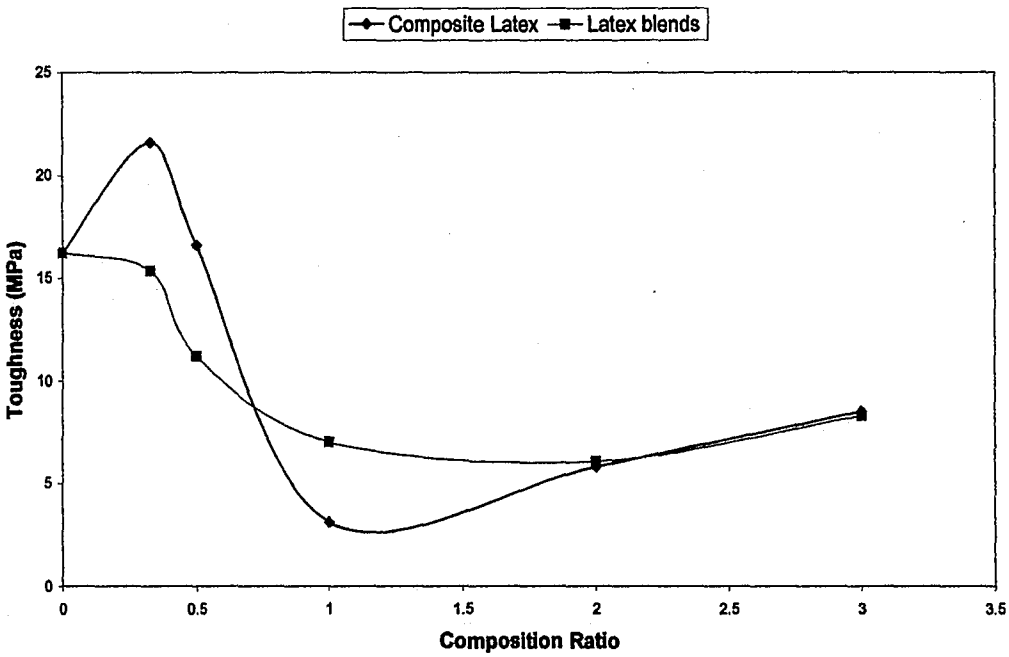

Figure 3-13: Latex film toughness versus composition ratio (core/shell)

Figure 3-13 shows a similar result to Figure 3-10 except the toughness is graphed for both latex blend and composite versus the compositional ratio of core polymer to shell polymer. Just as in figure 3-10, the toughness is the same initially for both blend and composite for compositions of 75/25 and 66/33. At 50/50, the blend begins to show improved toughness until it reaches compositions of 33/66 and 25/75, where the composite starts to exhibit greater toughness.

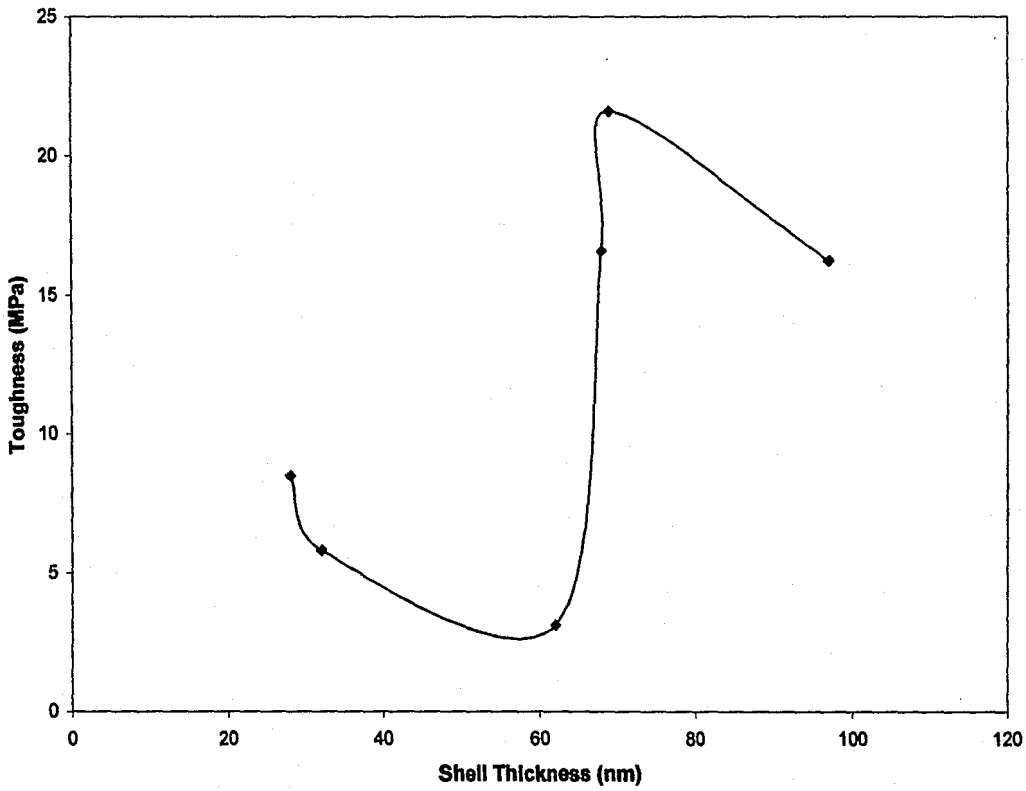

Figure 3-14: Shell thicknesses of the composite latex particles versus toughness (semi-continuous polymerization process).

Figure 3-14 shows the influence of the shell thickness of the composite latex particles on toughness for the series synthesized by semi-continuous polymerization without no crosslinker present. Initially, as the shell thickness increases, the toughness goes down slightly until the shell thickness reaches approximately 60 nm. At this point the toughness drastically increases and reaches a point where it appears to level off somewhat. The toughness increases very drastically at 60 nm with very small increases in shell thickness.

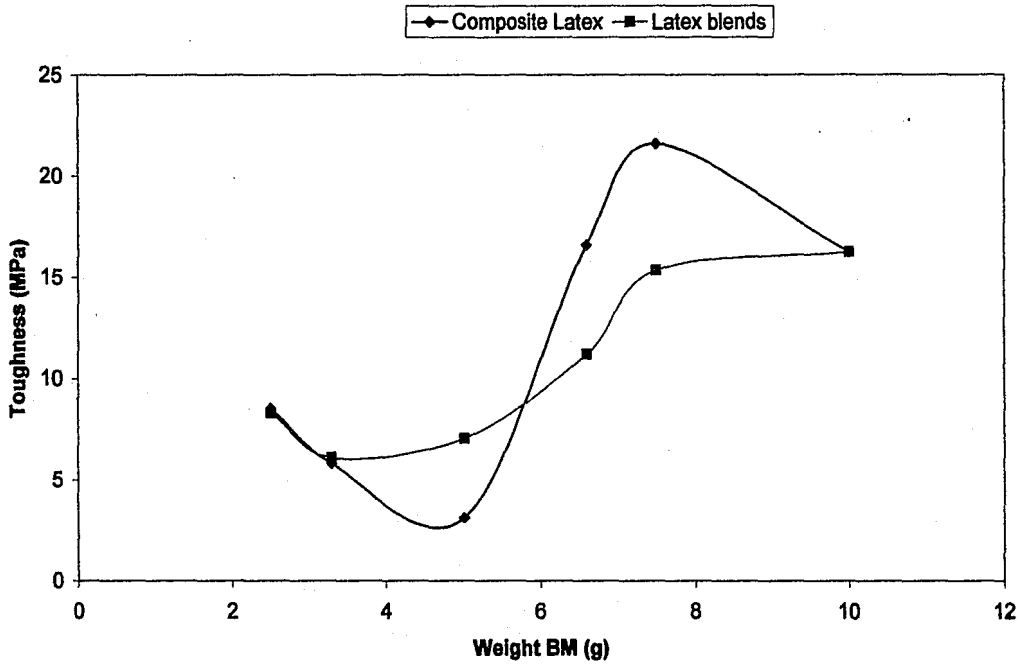

Figure 3-15: The weight of BM per latex particle versus toughness for the core/shell latex. The curve for the latex blend shows the amount of BM in the P2EHMA/BM component versus toughness

Figure 3-15 shows that the amount of BM has a greater overall effect in increasing toughness in the composite particles than in the blend except at the higher core/shell weight ratios. The amount of BM per latex particle is dependant on the amount of shell material used.

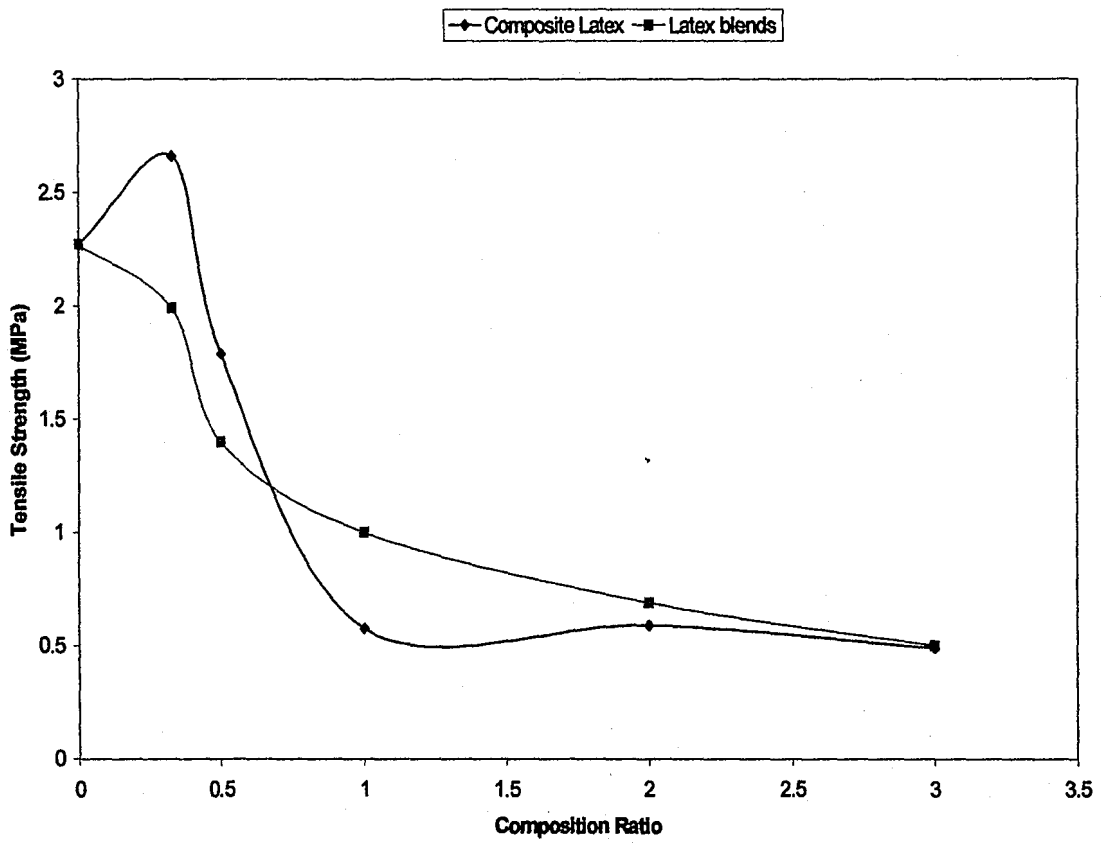

Figure 3-16: Tensile strength versus the core/shell weight ratio.

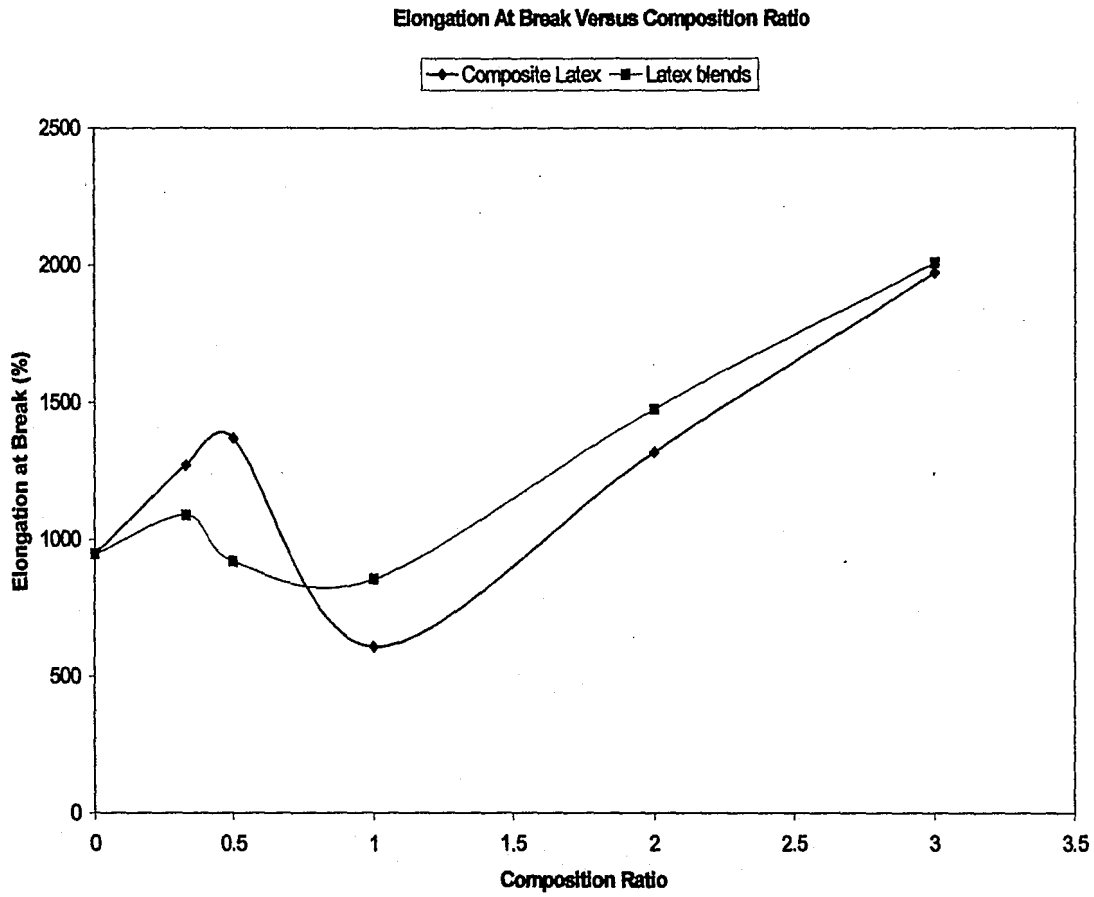

Figure 3-17: Elongation at break versus core/shell weight ratio.

Figures 3-16 shows a gradual decrease in tensile strength with increasing core to shell composition ratio. However, the elongation is gradually increasing with composition ratio as shown in figure 3-17. Figure 3-13 shows a similar trend.

Table 3-15 provides a direct comparison of the mechanical properties obtained from the 33/66 composite latex synthesized by the seed/swelling technique versus the semi-continuous polymerization technique.

Table 3-15: Comparison of the Mechanical Properties of Dried Latex Synthesized by the Seed/Swell Method Versus the Semi-Continuous Method

Sample PLMA/P2EHMA	Stress at break (MPa)	% Strain at break (MPa)	Modulus (MPa)	Toughness (MPa)	Maximum Strain (mm/mm)
Composite latexes					
33/66 seed/swell	1.80	1370.00	3.97	16.60	13.70
33/66 semi-cont.	1.15	1026.31	3.13	11.98	10.32
Latex blend					
33/66 blend	0.49	920.00	2.61	11.20	9.30

Table 3-15 shows that in all cases the mechanical properties of the latex blends are inferior to both types of composite latex particles regardless of the synthesis method that was employed. The seed/swell synthesis method yielded the highest mechanical properties overall in this comparison in terms of toughness and tensile stress at break. Perhaps better adhesion between the phases is achieved in the seed/swell method as opposed to the semi-continuous method. This adhesion may be due to some grafting reactions.

Table 3-16 shows the results of the mechanical properties obtained for the series of composite latex films synthesized with 1 wt% EGDMA crosslinker. The 0/100 sample was extremely brittle which caused the toughness and strain to be very low. Figure 3-18 shows how the toughness of the composite latex films varies with composition ratio. There appears to be a large increase in toughness with the 25/75 sample. This may have been due to some variation in the sample that occurred during compression molding. Variations in temperature or pressure during the molding cycle could cause variations in toughness.

Table 3-16: The mechanical properties of composite latex films synthesized with EGDMA crosslinker

Sample PLMA/P2EHMA	Stress at break (MPa)	% Strain at break (MPa)	Modulus (MPa)	Toughness (MPa)	Maximum Strain (mm/mm)
Composite latexes					
0/100	1.83	66.29	4.10	0.78	0.69
25/75	1.27	1027.00	4.60	9.19	10.33
33/66	0.73	401.10	3.78	2.68	4.22
50/50	0.64	839.30	0.65	4.27	8.72
66/33	0.50	790.00	0.40	3.69	7.91
75/25	0.13	762.02	0.31	1.28	9.10
Latex blends					
0/100	1.83	66.29	4.10	0.78	0.69
33/66	0.86	480.50	4.80	4.53	4.83
50/50	0.34	510.30	1.10	0.53	6.15

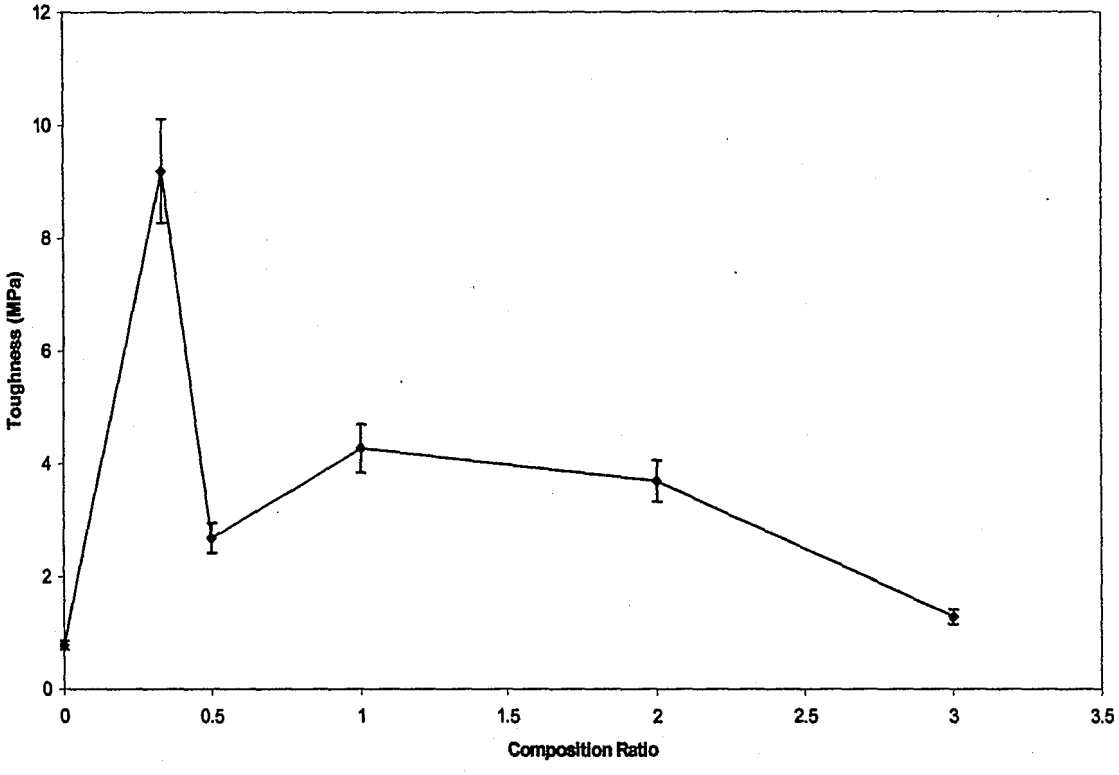

Figure 3-18: Composition ratio versus toughness of the composite latex films synthesized with 1% EGDMA crosslinker.

Figure 3-18 shows a similar trend where toughness initially increased then decreased as was seen in figure 3-13. However, in Figure 3-18 the toughness gradually decreases as the composition ratio increases, whereas in Figure 3-13 the toughness starts to increase slightly as the composition ratio increases.

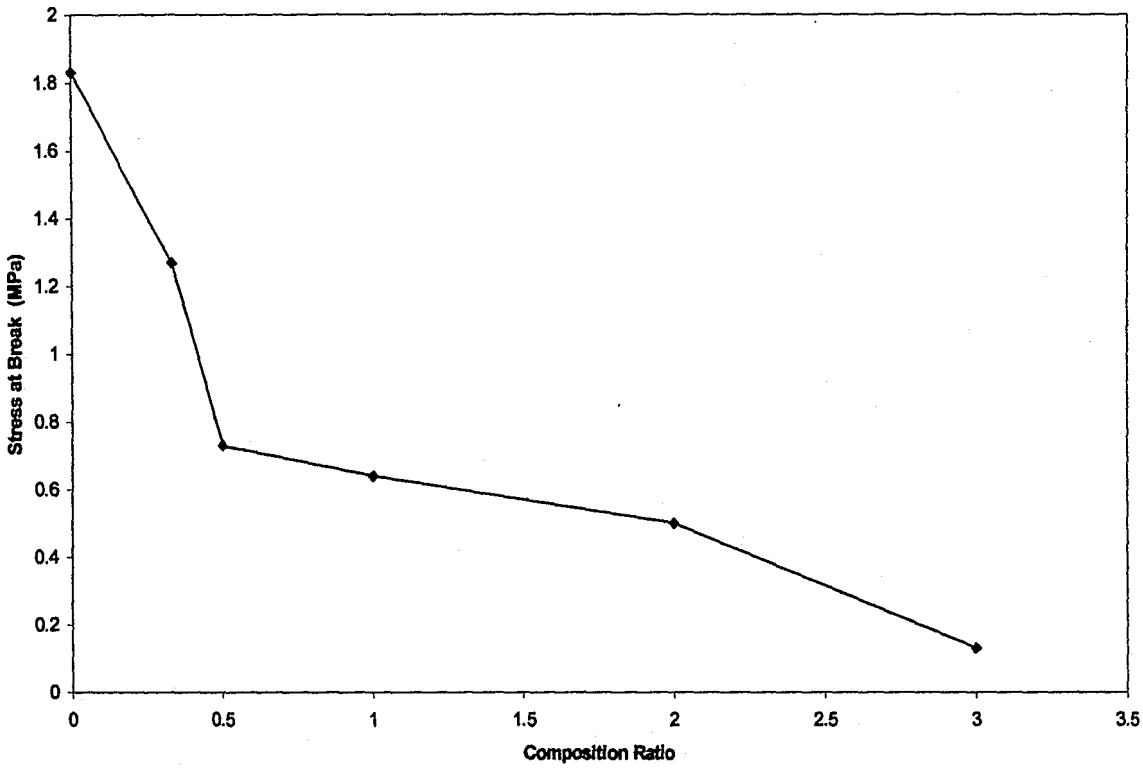

Figure 3-19: Composition ratio versus tensile stress at break for the core/shell latex films synthesized with 1% EGDMA crosslinker.

Figure 3-19 shows a continuous decrease in the tensile strength of the latex films with crosslinker. It was noticed that the films were considerably more brittle than the films prepared without crosslinker, which may account for the gradual decrease in tensile strength with composition ratio. Figure 3-20 shows a similar trend to that of (figure 3-18) the tensile strength.

Table 3-17 below summarizes the mechanical properties obtained for the series of composite core-shell latex synthesized by batch polymerization using 1 mM AIBN initiator in place of KPS in the second stage polymerization. The properties are plotted in Figures 3-21 through 3-23.

Table 3-17: Mechanical Properties of the Composite Core-Shell Latexes Synthesized with 1 mM AIBN Initiator

Sample PLMA/P2EHMA	Stress at break (MPa)	% Strain at break (MPa)	Modulus (MPa)	Toughness (MPa)	Maximum Strain (mm/mm)
Composite latexes					
25/75	1.25	652.00	2.00	6.20	6.60
33/66	1.59	1148.00	5.04	12.86	11.55
50/50	1.35	1392.10	1.76	12.70	13.90
66/33	0.45	995.12	0.34	3.33	10.79
75/25	0.31	836.72	0.29	2.07	9.24

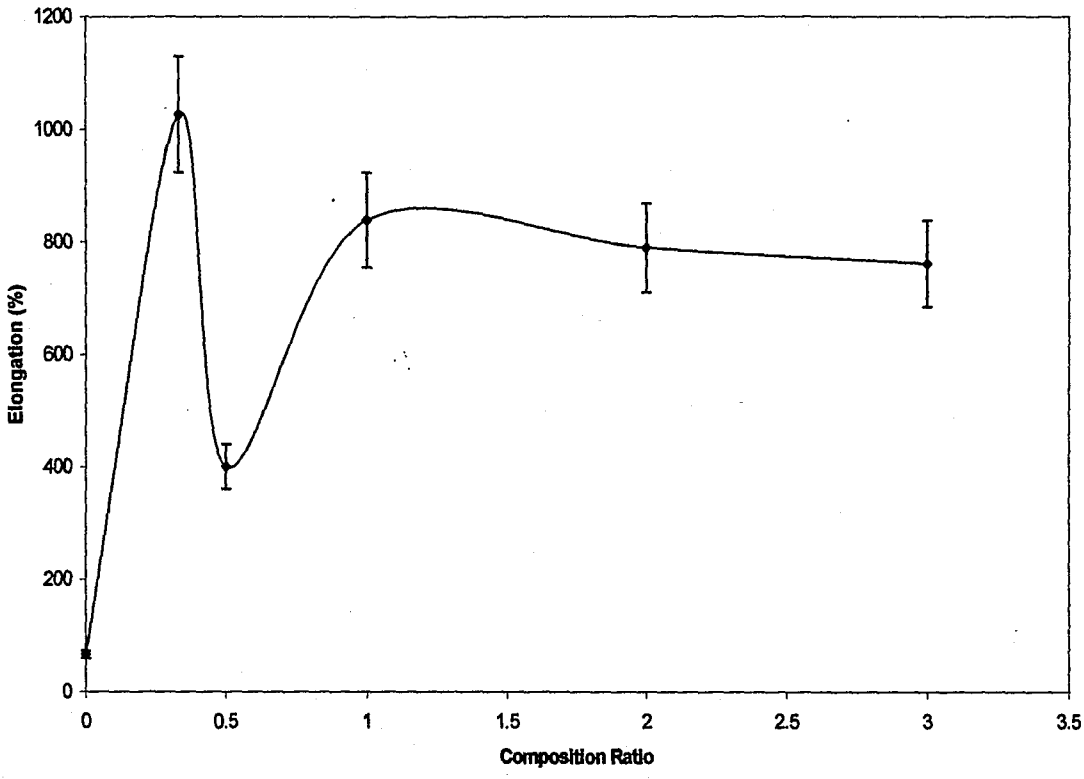

Figure 3-20: Elongation versus composition ratio for the latex films synthesized with 1% EGDMA crosslinker.

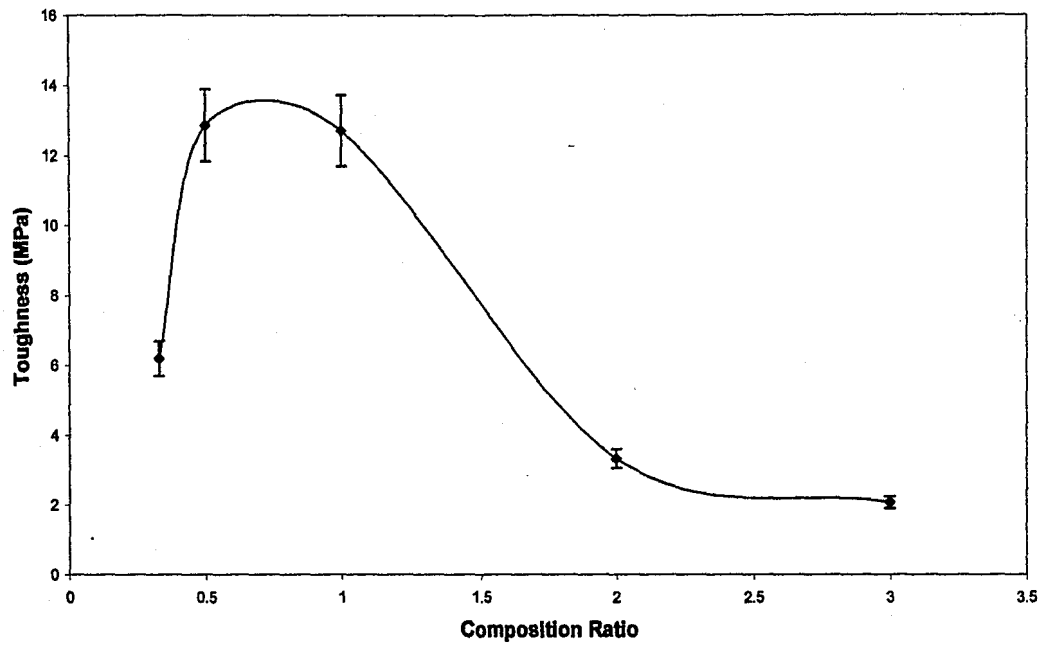

Figure 3-21: Toughness versus composition ratio for the series of composite latex particles synthesized by batch polymerization in the presence of 1 mM AIBN initiator.

Figure 3-21 shows a similar trend to that obtained in figure 3-13 for the series with KPS initiator except that the maximum toughness for these series differ considerably. The series with KPS has a higher maximum toughness at (25/75) of 22 MPa versus 13 MPa for the AIBN series. However, the maximum toughness in figure 3-21 is somewhat higher than in the series with crosslinker (12.86 versus 9.4).

Figure 3-22 shows that the tensile stress at break first increases slightly and then decreases as the composition ratio increases. This trend would be expected since the amount of the softer PLMA material over the higher T_g polymer (P2EHMA) is increasing in this range. Figure 3-23 shows that the elongation follows a similar trend as the tensile stress and toughness at break.

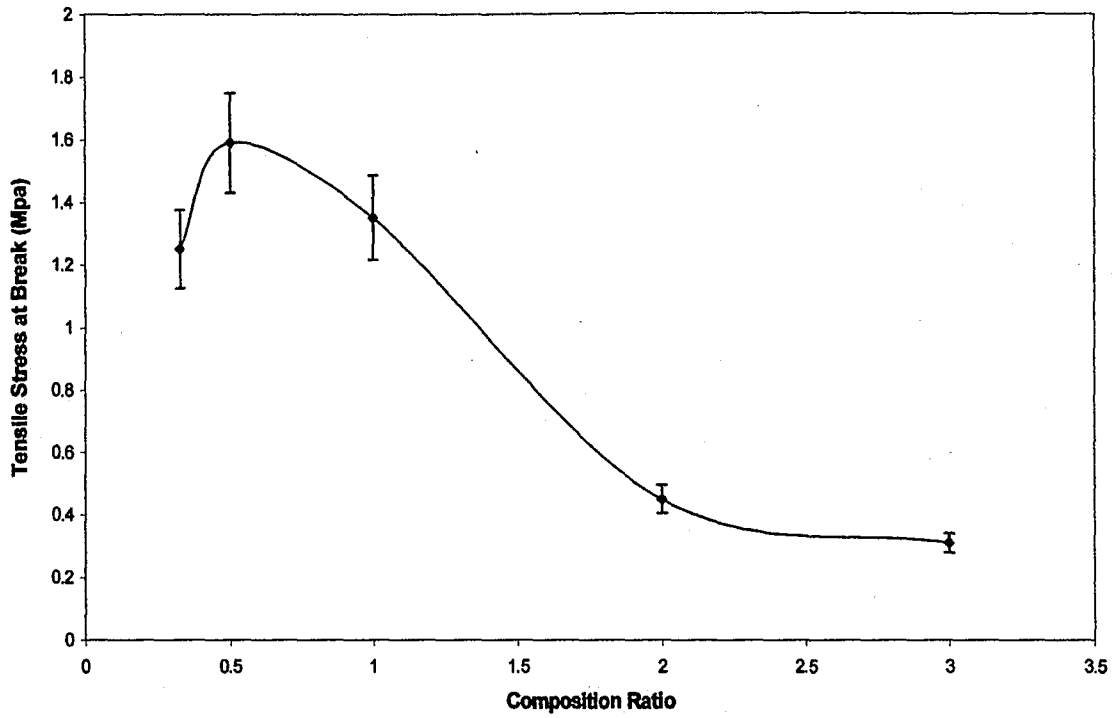

Figure 3-22: Tensile stress at break versus composition ratio for the series of composite latex particles synthesized by batch polymerization in the presence of 1 mM AIBN initiator.

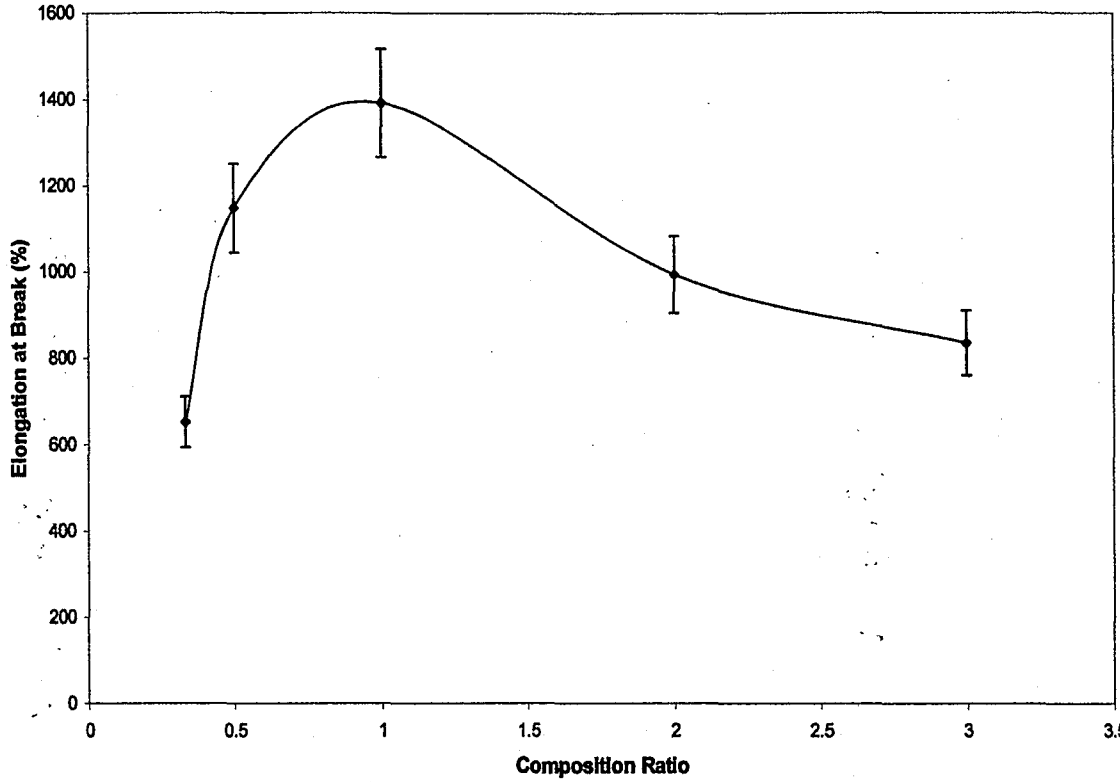

Figure 3-23: Elongation at break versus composition ratio for the series of composite latex particles synthesized by batch polymerization in the presence of 1 mM AIBN initiator.

3.7 Atomic Force Microscopy Studies (AFM)

Atomic force microscopy was employed to study the 33/66 wt% dried latex films. The AFM was used in noncontact mode. The AFM settings commonly used were: (1) oscillation frequency: 274 kHz; (2) amplitude: 35 V; (3) scan range: 1 μm; (4) scan rate: 0.98 μm/sec.; (5) resolution: 300; (6) peak to valley height: 124 nm.

Figure 3-24 shows topographical and phase images for the 33/66 wt% dried latex film synthesized by the seed/swell technique with no crosslinker. The film shown is not very uniform and it appears that some PLMA from some of the cores of the latex particles phase separated out of the shell portions of the particles. This could explain why some of the particles appear to have a "collapsed" shape. Additionally, some microdomains in the phase image of Figure 3-24 are evident on the surface of the latex particles. A peak to valley height measurement was made and a value of 124 nm was obtained. This number is smaller than what would be expected since the measured latex particle size was about 200 nm (by CHDF).

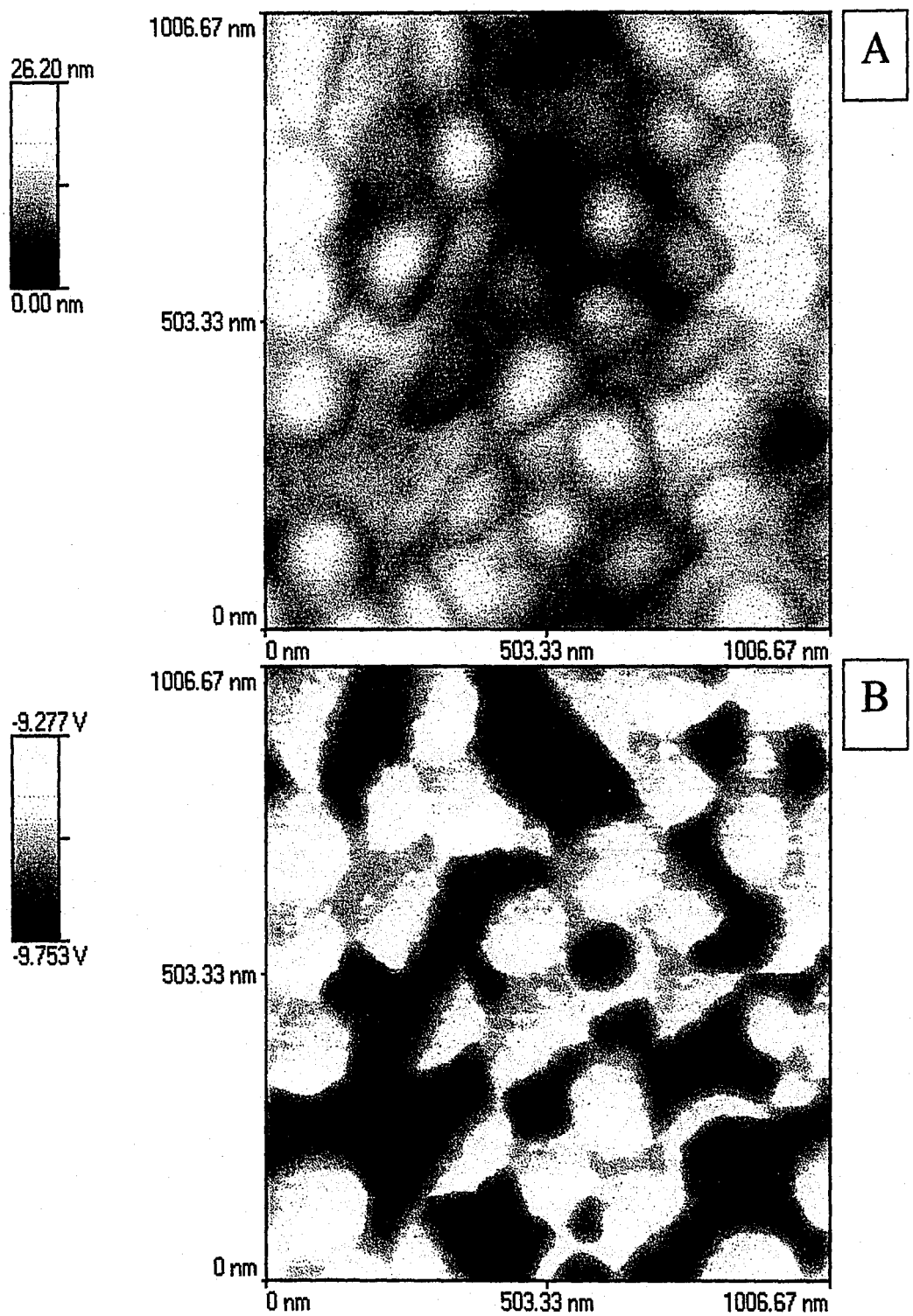

Figure 3-24: (A) Topographical and (B) Phase images of the dried 33/66 wt% core-shell latex film synthesized by the seed/swell technique without crosslinker.

Figure 3-25 shows the corresponding 33/66 wt% latex blend. Some interstitial spaces in between groups of latex particles are evident which could contain another material such as surfactant. Perhaps the coalescence of latex was not fully complete in this film.

Figure 3-26 shows the AFM results for the 33/66 composition latex film synthesized by semi-continuous polymerization. The shell portions of the latex particles were not evident here. This may have been due to swelling of the shell material with monomer during the second stage polymerization. It is possible that some PLMA from the cores phase separated out to the particle surfaces during film formation, which could occur if the shells opened. The particles may be buried in the core PLMA polymer or surfactant or a combination thereof. The material in the gaps of the film is about 10 nm in height. There are no microdomains of shell material evident here. Figure 3-27 shows 3-D images of the film synthesized by batch polymerization (lower image) compared to the film synthesized by semi-continuous polymerization. These images indicate that the film surface in image B has a higher degree of uniformity in its surface morphology than the one shown in A. The latex particles kept their integrity more in the film in image B than in image A.

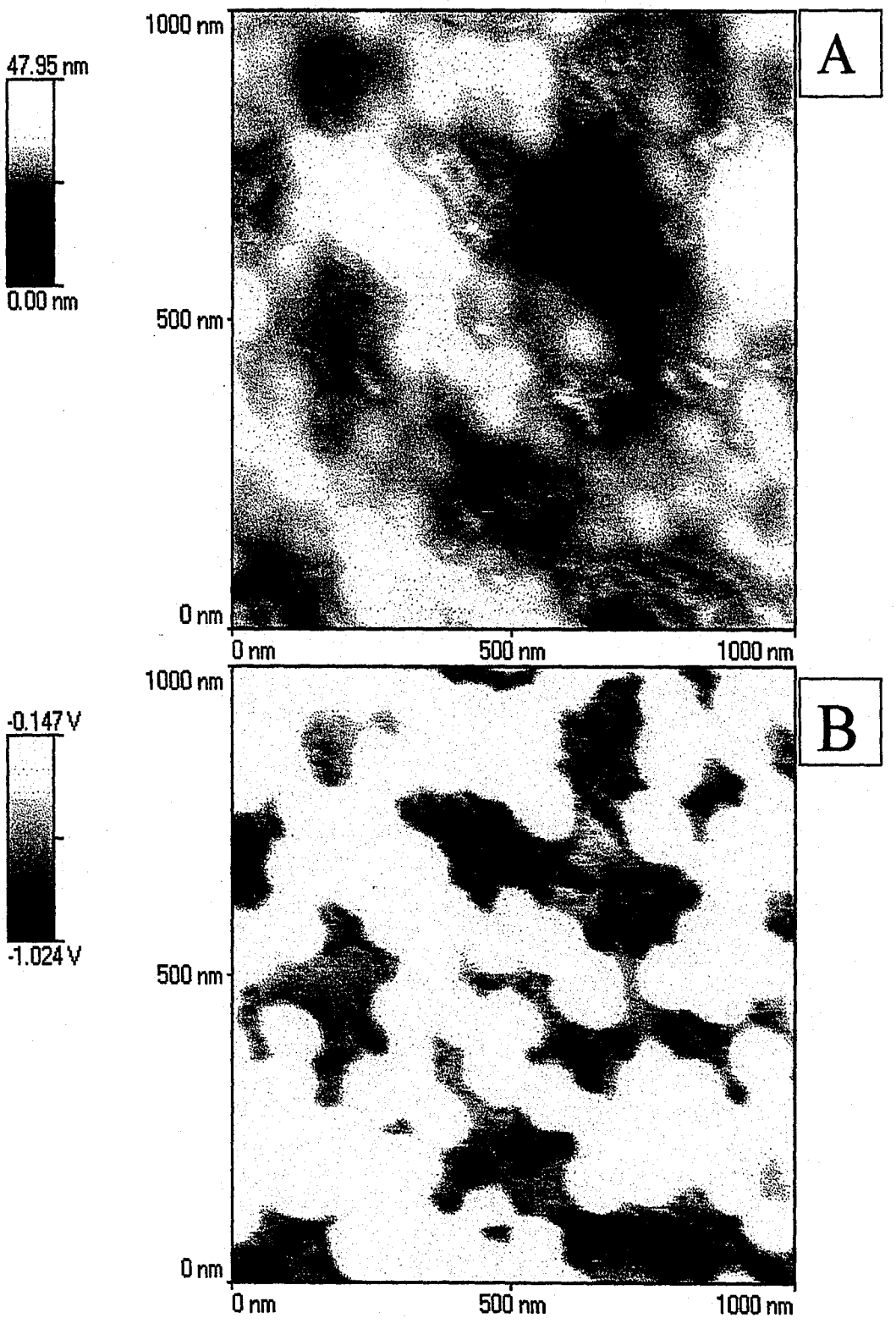

Figure 3-25: AFM topographical (A) and phase (B) images of the dried 33/66 wt% ratio latex blend film.

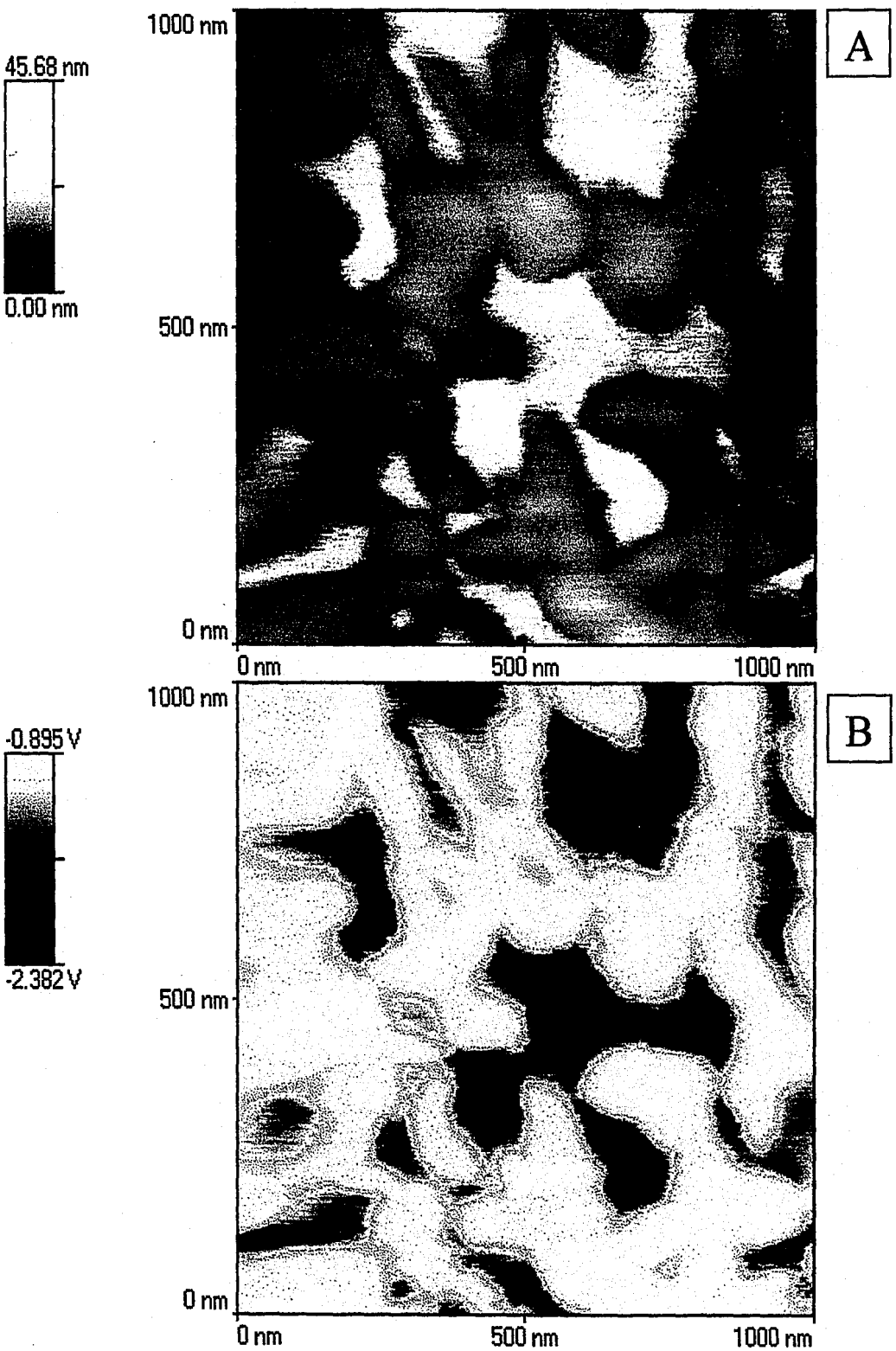

Figure 3-26: (A) AFM topographical and (B) phase images of the 33/66 composition ratio core-shell latex film synthesized by semi-continuous polymerization.

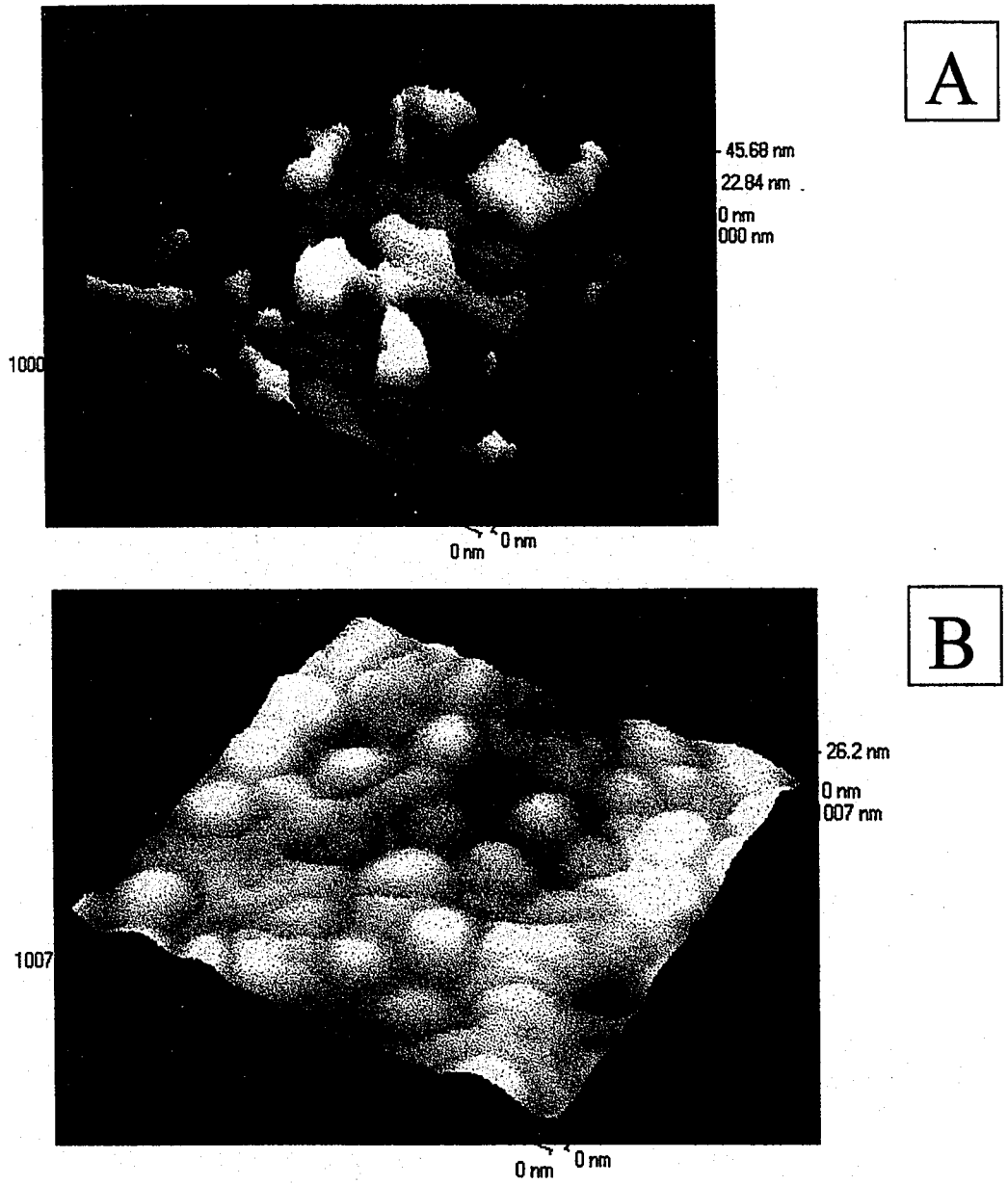

Figure 3-27: (A) AFM three-dimensional image of 33/66 wt% core-shell PLMA/P2EHMA-BM latex film synthesized by semi-continuous polymerization, corresponding to Figure 3-26 (2-D image). (B) AFM three-dimensional image of the 33/66 wt% core-shell latex film synthesized using the seed/swell technique corresponding to Figure 3-24 (2-D image).

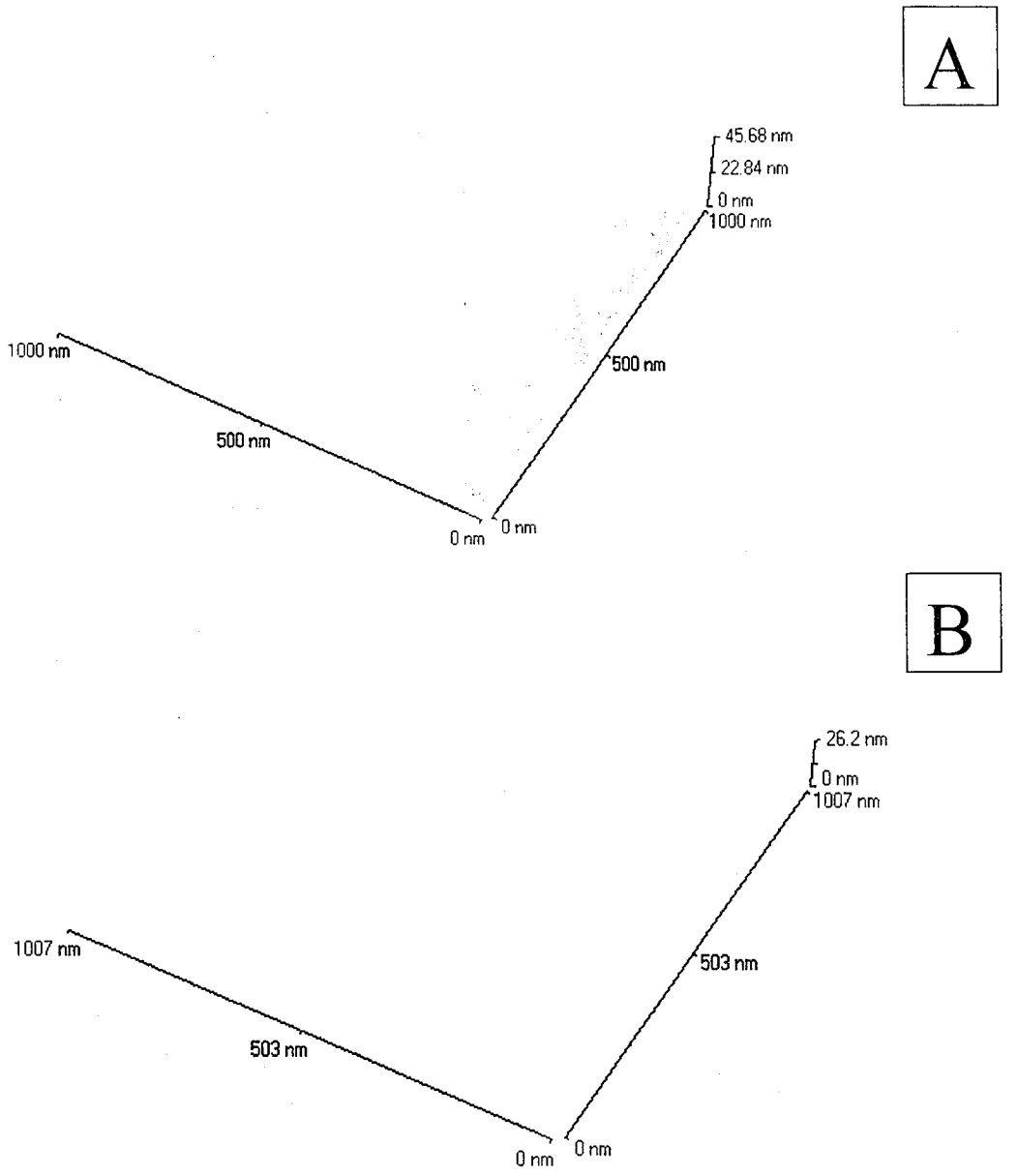

Figure 3-27: (A) AFM three-dimensional image of 33/66 wt% core-shell PLMA/P2EHMA-BM latex film synthesized by semi-continuous polymerization, corresponding to Figure 3-26 (2-D image). (B) AFM three-dimensional image of the 33/66 wt% core-shell latex film synthesized using the seed/swell technique corresponding to Figure 3-24 (2-D image).

Figure 3-28 shows topographical and phase images of the latex film synthesized with EGDMA crosslinker in the P2EHMA phase. These images show that these particles maintained their integrity after film formation and no contents of core material appeared to be released as was postulated for the film shown in Figure 3-26. The dark color in the gaps between the particles could possibly be small amounts of homopolymer or surfactant. Since most of the surfactant ends up at the edges of the dried film, the edges were avoided in these images. However, it is possible that the area chosen for these images were not adequately far from the edges of the film.

Figure 3-29 shows the topographical and phase image results for the 33/66 dried latex film synthesized in the presence of 1 mM AIBN initiator in the second stage polymerization. This film exhibited very good packing of the latex particles and appeared to be more uniform in structure. In addition, it was noticed in the various images that were obtained from this film (some are not shown here) that the particles (in a qualitative sense) appeared very monodisperse in particle size distribution. The particles appeared to be somewhat smaller than in the films shown in the previous images. Additionally, the films prepared with the AIBN initiator, qualitatively appeared to have the highest gloss. A small amount of microdomains was evident in figure 3-29; however, not to the same extent as that seen in Figure 3-24. Figure 3-30 shows the AFM results of the same film as in Figure 3-29 except the area of study was at the edge of the film. It was determined that the dark regions correspond to a soft material, perhaps PLMA. The close packing of the latex was the same at the edge as in the center region of the film.

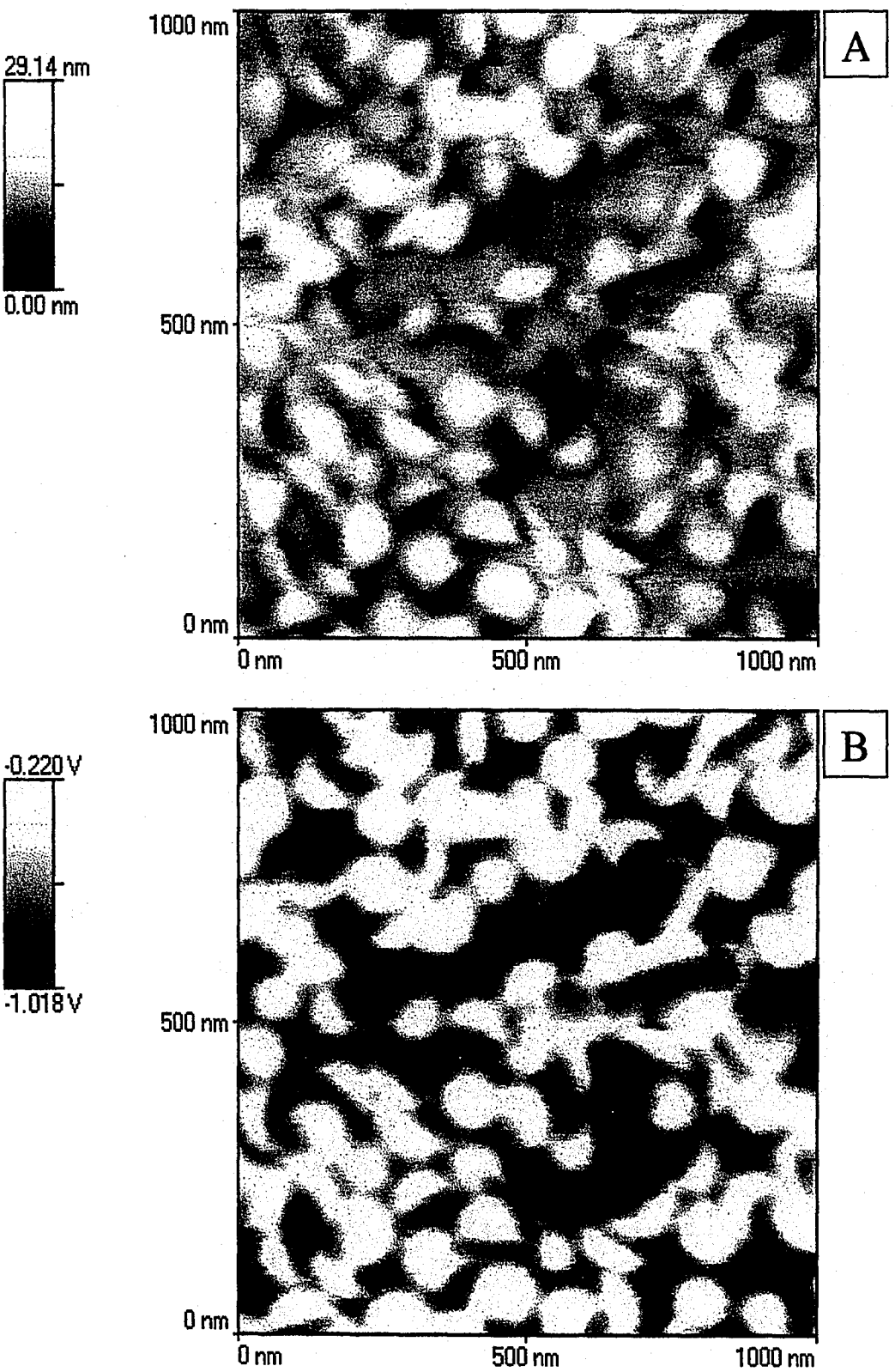

Figure 3-28: (A) AFM topographical and (B) phase images of the 33/66 wt% core-shell latex film synthesized with 1 wt% EGDMA crosslinker based on monomer.

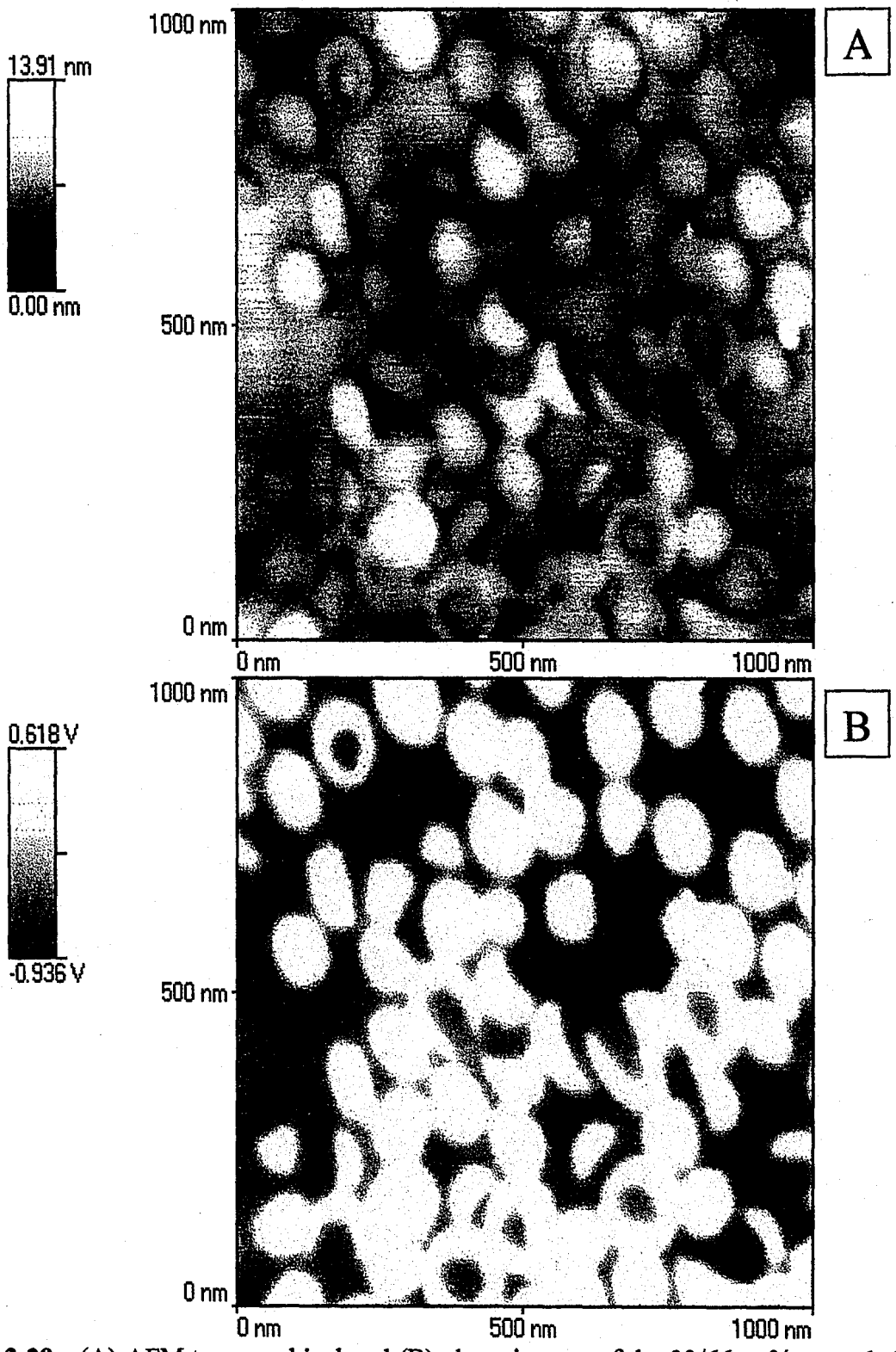

Figure 3-29: (A) AFM topographical and (B) phase images of the 33/66 wt% core-shell latex film synthesized in the presence of 1 mM AIBN initiator in place of KPS. The area of study here was at the **center** of the dried film.

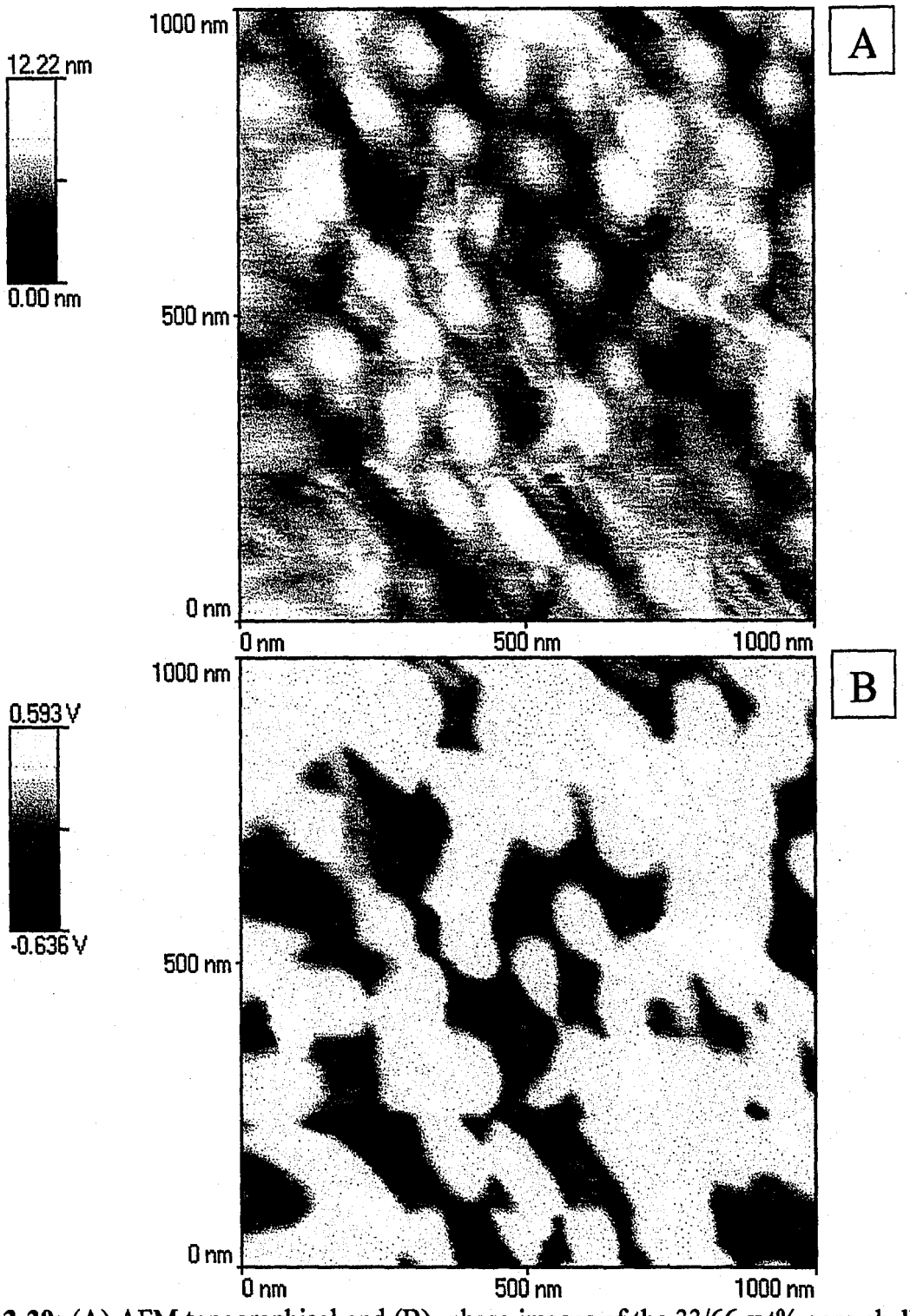

Figure 3-30: (A) AFM topographical and (B) phase images of the 33/66-wt% core-shell latex film latex film synthesized in the presence of 1 mM AIBN initiator in place of KPS. This is the same film as shown in Figure 3-29, except the area of study is at the **edge** of the film.

This close packing and higher uniformity in particle size may explain why the mechanical properties of this film were somewhat better than those obtained from the latex blend, the semi-continuous films and even the film with EGDMA crosslinker. Only the films synthesized by the seed/swell technique showed superior physical properties in comparison to this series.

The films produced by the seed/swell technique yielded the best mechanical properties overall compared to all the other types of films produced here. Perhaps some of the microstructure found on the surfaces of the particles helped to strengthen the films acting as areas of physical crosslinking between latex particles. The microstructure may have aided in the coalescence process by increasing the overall surface area of the particles that contact each other.

The series with crosslinker present had the poorest mechanical properties. This may have been due to the rather large gaps that appeared in the image in Figure 3-28 between adjacent latex particles. Perhaps the surface area and size of the gaps could be estimated in some way. In addition, it appears that the coalescence process had not progressed to as great an extent as that seen in the other films.

CHAPTER 4

CONCLUSIONS

Seed latexes of PLMA were synthesized via batch polymerization. Core-shell latexes of low T_g can be synthesized by a seed/swell technique and a semi-continuous polymerization technique. The P2EHMA phase (shell) can be crosslinked with EGDMA.

The results of glass transition measurements on the films of composite latexes synthesized here indicate very little change in T_g as compared to the measurements made on PLMA homopolymer and P2EHMA/BM copolymer. The indication is that these two polymers are not very miscible with one another. The T_g did increase somewhat in the P2EHMA phase when crosslinker was added. Therefore, a lightly crosslinked phase was achieved when EGDMA was added. The T_gs obtained from the semi-continuous process appeared broader than those obtained in the seed/swell process. This may indicate that greater miscibility between the two phases is achieved in the semi-continuous process.

The mechanical properties obtained for the 33/66 wt% series of latexes were superior overall to those obtained by simple physical blending except in the case where EGDMA crosslinker was added. The greatest improvement in properties as compared to the latex blends was seen with the latex synthesized by the seed/swell technique. The other synthesis techniques such as semi-continuous and AIBN initiator showed only modest improvements in these properties. For these films the toughness and elongation at

break were relatively close to those obtained with the latex blend except the tensile stress at break.

Results of AFM studies were employed to correlate physical properties measured with latex film structure on a microscopic scale. The images obtained for the seed/swell film indicated microstructure and rather complete coalescence. Voids or gaps between latex particles were qualitatively smaller than in the other films. All of which led to an increase in mechanical film strength compared to the other films tested.

REFERENCES

1. P.M. Lesko and P.R. Sperry," Acrylic and Styrene-Acrylic Polymers" in *Emulsion Polymers and Emulsion Polymerization*, P.A. Lovell and M.S. El-Aasser, Eds., John Wiley and Sons, Ltd., New York, pp. 619-651 (1997).

2. V.L. Dimonie, E.S. Daniels, O.L. Shaffer and M.S. El-Aasser," Control of Particle Morphology" in *Emulsion Polymers and Emulsion Polymerization*, P.A. Lovell and M.S. El-Aasser, Eds., John Wiley and Sons, Ltd., New York, pp. 293-323 (1997).

3. W.D. Hergeth, K. Schmutzler and S. Wartewig, *Makromol. Chem., Makromol. Symp.*, **31**,123-142 (1990).

4. J. Feng, M.A. Winnik, R. Shivers, and B. Clubb, *Macromolecules*, **28**, pp.7671-7682 (1995).

5. S. Lepizzera, C. Lhommeau, G. Dilger, T. Pith, and M. Lambla, *Journal of Polymer Science: Part B: Polymer Physics*, **35**, pp. 2093-2101 (1997).

6. R.M. Rynders, C.R. Hegedus and A.G. Gilcinski, *Journal of Coatings Technology*, **67**, No. 845,pp. 59-68 (1995).

7. A.S. Dunn,"Harkins, Smith-Ewart and Related Theories" in *Emulsion Polymers and Emulsion Polymerization*, P.A. Lovell and M.S. El-Aasser, Eds., John Wiley and Sons, Ltd., New York, p. 143 (1997).

8. A.S. Dunn,"Harkins, Smith-Ewart and Related Theories" in *Emulsion Polymers and Emulsion Polymerization*, P.A. Lovell and M.S. El-Aasser, Eds., John Wiley and Sons, Ltd., New York, p. 137 (1997).

9. R. Z. Greenly, in *Polymer Handbook*, 3rd edn, J. Brandrup and E.H. Immergut (eds), Wiley-Interscience, New York, 1989.

10. R. Z. Greenly, in *Polymer Handbook*, 3rd edn, J. Brandrup and E.H. Immergut (eds), Wiley-Interscience, New York, p. 342 ,1989.

11. L.E. Nielsen and R.F. Landel, *Mechanical Properties of Polymers and Composites*, 2nd edn, Marcel Dekker, New York, p.19-20 (1994).

12. L.H. Sperling, *Polymer Multicomponent Materials*, John Wiley & Sons, New York, p. 25-26 (1997).

VITA

Karl received a Bachelor of Science degree in physics from Allegheny College in 1989. He joined Thomas & Betts Corporation in 1995 where he worked as a materials project scientist until 1999. He began pursuing a Master's of Science degree in 1997 as a graduate student and joined the Emulsion Polymers Institute in 1999. He is currently employed at Kensey Nash Corporation as a polymer chemist working in the field of bio-absorbable polymers.

END OF TITLE